

ADSORPTION OF HUMAN SERUM ALBUMIN TO POLYSTYRENE LATEX
GRAFTED WITH N,N- DIMETHYLACRYLAMIDE

by

FARHAD RAMEZANI

B.Sc. Hons., University of British Columbia, 1996

A THESIS SUBMITTED IN PARTIAL FULFILLMENT
OF THE REQUIREMENTS FOR THE DEGREE OF
MASTER OF SCIENCE

in

THE FACULTY OF GRADUATE STUDIES

Department of Pathology and Laboratory Medicine

We accept this thesis as conforming
to the required standard

THE UNIVERSITY OF BRITISH COLUMBIA

May 1999

© FARHAD RAMEZANI, 1999

In presenting this thesis in partial fulfilment of the requirements for an advanced degree at the University of British Columbia, I agree that the Library shall make it freely available for reference and study. I further agree that permission for extensive copying of this thesis for scholarly purposes may be granted by the head of my department or by his or her representatives. It is understood that copying or publication of this thesis for financial gain shall not be allowed without my written permission.

Department of Pathology and Laboratory medicine

The University of British Columbia
Vancouver, Canada

Date 07/JUNE/1999

Abstract

Biocompatible materials can be defined as materials which can be introduced into a living organism without producing stress or traumatic response. When a solid material comes in contact with a biological medium, a layer of protein immediately binds to the surface. Subsequent defensive responses depend on the type and binding orientation of the protein on the surface. Therefore, primary surface protein binding is directly related to the type of physiological response observed in the body.

Surfaces coated with grafted hydrophilic polymers can reduce non-specific protein adsorption. The hydrophilic nature of the grafted chain reduces the hydrophobic driving force. The long grafted chains extending out through the electrical double layer can reduce electrostatic driving forces. Non-specific protein can be excluded by the grafted chains and the solvent trapped between grafted chains.

Polymer chains of hydrophilic poly(N,N -dimethylacrylamide) of different lengths were polymerized *in situ* by initiation from aldehyde groups on the surface of polystyrene latex. Using the techniques of particle electrophoresis, conductometric titration and elemental analysis, the surfaces of these latexes were analyzed. The adsorption isotherms of human serum albumin (HSA) to these latexes were measured. The results indicate that HSA has an affinity for the grafted poly(N,N -dimethylacrylamide). The exclusion effect of the grafted polymer in reducing HSA adsorption was greatest with the medium length grafted chains. The shorter or longer grafted chains on the latex did not reduce HSA adsorption compared with non-grafted latex.

Tables of Contents

Abstract.....	II
Table of contents.....	III
List of figures.....	V
List of tables.....	VII
Acknowledgments.....	VIII
Dedication.....	IX
1. Introduction.....	1
1.1. Overview.....	1
1.2. Protein Structure.....	2
1.3. Human Serum Albumin.....	4
1.4. Principle of Colloid Stability.....	5
1.5. Interaction of Blood Proteins and Artificial Surfaces.....	9
1.6. Thermodynamics of Protein Adsorption.....	10
1.7. Surfaces with a Grafted Hydrophilic Polymer as Biocompatible Surface.....	12
1.8. Conformation of the End-Grafted Chains on a Surface.....	13
1.9. Theoretical Model to Study Interaction of a Brush polymer with a Protein.....	15
1.10. Size Exclusion Properties of the Brush Polymer.....	18
2. Polystyrene Latex Synthesis and Grafting of Poly(2-methoxyethylacrylate) and Poly(<i>N,N</i> -dimethylacrylamide).....	21
2.1. Polystyrene Latex Synthesis.....	21
2.2.1 Materials.....	21
2.2.2 Synthesis Method.....	22
2.2.2.1 Synthesis of Latex Seed.....	22
2.2.2.2 Seeded Polymerization.....	22
2.2.2.3 Acrolein/ Styrene Copolymer Shell.....	23
2.2.3 Analysis Methods.....	24
2.2.3.1 Size Distribution of Latex.....	24
2.2.3.2 Surface Charge Density.....	24
2.2.3.3 Aldehyde Content of Copolymer Shell.....	26
2.2.3.4 Electrophoretic Mobility.....	27
2.2.3.5 Results.....	27
2.2.4 Discussion.....	29
2.2.5 Conclusion.....	32
2.2 Ce(IV) Initiated Graft Polymerization.....	32
2.2.1 Introduction.....	32
2.2.2 Materials.....	34

2.2.3	Methods.....	34
2.2.4	Results.....	35
2.2.4.1	Ce(IV) Initiated Grafted Polymerization of 2-methoxyethylacrylate(MEA).....	35
2.2.4.2	Ce(IV) Initiated Grafted Polymerization of N,N -dimethylacrylamide.....	39
2.2.5	Discussion.....	43
2.2.6	Conclusion.....	46
3.	Adsorption of Human Serum Albumin on the Grafted Latex.....	48
3.1	Adsorption Isotherm.....	48
3.1.1	Introduction.....	48
3.1.2	Materials.....	48
3.1.3	Methods.....	49
3.1.3.1	Human Serum Albumin Labeling with Iodine-125.....	49
3.1.3.2	Human Serum Albumin Stock Preparation.....	50
3.1.3.3	HSA Adsorption to the Latex Grafted with N,N -dimethylacrylamide.....	51
3.1.4	Results.....	53
3.1.5	Discussion.....	57
3.2	The Nature of Adsorption of HSA to Poly(N, N dimethyacrylamide).....	60
3.3	Conclusion.....	63
	Entropic Interaction Chromatography with Poly(N, N dimethylacrylamide) Grafted Latex.....	64
4.1	Introduction.....	64
4.2	Materials and Methods.....	64
4.3	Results.....	65
4.4	Discussion.....	67
4.5	Conclusion.....	67
6.	Thesis Conclusion.....	68
	References.....	69
	Appendix.....	78

List of Figures

Figure 1.1: Schematic representation of the electrical double layer.....	7
Figure 1.2: Brush-Particle interaction energy curves as a function of position.....	17
Figure 2.1: Positively charged poly(styrene) latex.....	25
Figure 2.2: Mechanism of Ce (IV) initiated graft polymerization.....	33
Figure 2.3: Hydrolysis of the 2-methoxyethylacrylate in an acidic medium.....	36
Figure 2.4: Microelectrophoretic mobility measurement of the polystyrene latex (diameter = 0.79 μm) before and after the grafting with N,N -dimethylacrylamide....	41
Figure 2.5: Microelectrophoretic mobility measurement of the polystyrene latex (diameter = 3.55 μm) before and after the grafting with N,N -dimethylacrylamide....	42
Figure 3.1: Human serum albumin adsorption to latexes by depletion method.....	54
Figure 3.2: Human serum albumin adsorption to by direct method in microhematocrit capillary tubes.....	55
Figure 3.3: Plot of supernatant counts (cpm/ml) vs wash number for HSA adsorbed to the latex FS4P2P'AG at two different concentration (washed with PBS and SDS).....	61
Figure 3.4: Plot of pellet counts (cpm/ml) vs wash number for HSA adsorbed to the latex FS4P2P'AG at two different concentration (washed with PBS and SDS).....	62
Figure 4.1: Saturation of the FS4P2P'AG with HSA(1 mg/ml).....	65
Figure 4.2: Entropic interaction chromatography with the polystyrene latex grafted with N, N dimethylacryamide.....	66
Figure A.1: Coudicometric titration of latex FS3A to determine amount of aldehyde groups on the surface.....	79
Figure A.2: Calibration curve of the grafted latex in microhematocrit capillary tube; weight of latex (FS3AG) vs volume fraction.....	82

Figure A.3: Human serum albumin adsorption to latexes by the direct method (pellet counts).....83

Figure A.4: Plot of HSA eluted from the column vs HSA applied to the column.....84

List of Tables

Table 2.1: Characterization of the seed latexes with or without acrolein shells.....	28
Table 2.2: Ce (IV) initiated grafting of 2-methoxyethylacrylate at different concentration of monomer, aldehyde and initiator.....	38
Table 2.3: Ce (IV) initiated grafting of 2-methoxyethylacrylate at different concentration of monomer, retarder (phenothiazine) and initiator.....	39
Table 2.4: Characterization of polystyrene latexes grafted with N,N -dimethylacrylamide.....	40
Table 3.1: Dissociation constants K_d and absorption maxima n for latexes by direct and depletion methods.....	55
Table A.1: Nitrogen analysis of non-grafted (blank) and grafted latex.....	79

Acknowledgments

I would like to thank Dr. Donald Brooks for giving me the opportunity to do this Master's thesis. I also appreciate his guidance and patience throughout this work. I would also like to thank Dr. Johan Janzen for his assistance with protein labeling, adsorption experiments and above all for his stimulating discussions. A special thanks goes to Raymond Norris-Jones for being a helpful friend. I am also grateful to the Medical Research Council of Canada for financial support.

To my family, friends

CHAPTER 1: Introduction

1.1 Overview

The surface chemistry, charge, wettability and topography of a potentially biocompatible material are all important factors to consider when trying to understand what occurs when it is used in contact with biological systems. The biological response starts with the interaction of proteins from a body fluid (e.g. blood, lymph or tears) with the surface of the material. The adsorption of protein can initiate activation of complement, platelets or macrophages which consequently may result in rejection of the synthetic material.

It has been shown that the surface modification of polymeric materials by immobilization of heparin directly or via a tether to the surface (1,2) increases the biocompatibility of the synthetic surface. Heparin is a polysaccharide which increases thromboresistance of the surface by binding to antithrombin and accelerating the antithrombin dependent inactivation of the blood coagulation proteases thrombin and factor Xa (3). Coating of the surface with cross-linked hydrophilic polymers like polyacrylamide increases biocompatibility by increasing lubricity and water content (4). Coating the surface with grafted hydrophilic polymer (5) or coating the surface with grafted macromolecules like poly(ethylene glycol) also increase biocompatibility by reducing protein adsorption (6). Other modifications such as surfaces with special patterns or textures (7,8,9), surfaces with self assembled monolayers (10) and multifunctional surfaces which mimic receptor sites (11) have also been shown to increase biocompatibility. Most recently, surface modification has been targeted to affect properties like lubricity (12), resistance to protein adsorption (13), enhancement

of protein adsorption (14, 15), protein retention (16), inhibition of cell adhesion (17) and enhancement of cell attachment and growth (18).

Designing a truly biocompatible surface requires a complete understanding of all the reactions that occur on the surface. For materials in contact with blood, these reactions are very complex due to the interaction of a wide range of blood proteins with the synthetic material. One approach is to investigate these surface interactions with simple systems of one or two proteins using theoretical models. Such theoretical models should enable us to make predictions about more complex protein-surface interactions. The purpose of this thesis is to study the interaction of protein with a surface grafted with brush polymers. Polystyrene latex particles grafted with poly(*N,N*-dimethylacrylamide) were synthesized and grafted polymer chain length and chain density estimated. The adsorption of human serum albumin (HSA) to the grafted latex was measured and analyzed by theoretical models, Flory- Huggins Mean Field Theory and numerical Self-Consistent Field Theory. The objective of this work is to better understand the mechanism of protein adsorption on the surface of synthetic materials grafted with a hydrophilic polymer and the effect of grafted chains in reducing protein adsorption. Latex grafted with *N,N*-dimethylacrylamide was evaluated for suitability as a size exclusion chromatography media.

1.2 Protein Structure

The primary structure of proteins, i.e. the amino acid sequence, determines the secondary structure or local spatial arrangements of the polypeptide's backbone atoms. This is due to hydrogen bonding, causing a regular polypeptide folding pattern

including helices, pleated sheets and turns. The tertiary structure of a protein is the overall molecular shape and three dimensional arrangement; that is, the folding of the secondary structural elements with the spatial arrangement of the side chains. Some of the forces responsible for the tertiary structure of proteins are electrostatic interactions, hydrogen bonding, hydrophobic interactions, salt bridges and covalent disulfide bonds. The main driving force involved in protein folding is the hydrophobic interaction between hydrophobic amino acids residues (19) and is due to the entropy increase of the ordered water which is released from the surface of the amino acid residues. The main opposing force to this folding is the entropy decrease due to changes in the rotational freedom of the peptide bonds. The difference between these two forces is small. Thus energetically, the overall folding of the protein on itself is marginally favourable (96). This also means the tertiary structure of proteins is usually very sensitive to changes in the temperature, pH or the presence of an interface. The favorable hydrophobic interactions of protein in aqueous solvent locates the non-polar amino acids like Val, Leu, Ile, Met into the non-polar interior, out of contact with the aqueous solvent. The charged polar amino acids Arg, His, Lys, Asp are largely located on the surface of a protein in contact with aqueous solvent. Any charged groups in the interior of a protein occur in ion pairs and are commonly involved in the catalytic activity of the protein, if present. The quaternary structure of the protein is the association of the independent tertiary structure (subunits) through hydrophobic interaction, hydrogen bonding and in some cases, inter-chain disulfide bonds.

1.3 Human Serum Albumin (HSA)

Human serum albumin consists of a single polypeptide chain of 585 amino acids, cross-linked and stabilized by 17 disulfide bonds (20). It is a 66 kDa monomeric protein which comprises almost 50 percent of the total protein in blood. Models based on amino acid sequencing predict that albumin molecules are composed of nine double loops linked together by short chains of amino acids (21). These nine double loops are not organized independently but are folded into three structural domains each having two large double loops with a small double loop between them (22). Crystallographic investigation of the three dimensional structure of albumin demonstrated the presence of three rather than nine structural domains (23).

The tertiary structure of the albumin is pH and temperature dependent. It has been shown that albumin is most stable at pH 6-7 and a temperature just below 5°C (24-27). When the pH is reduced to 3.4-3.6, the bonds between albumin domains are broken and the molecule undergoes a reversible expansion as a result of which the sedimentation coefficient, diffusion constant, intrinsic viscosity and the number of the interchangeable hydrogen atoms changes (24-27). This transformation of albumin due to lowering of the pH is called N-F transformation (N for normal and F for faster migration) (25). During N-F transformation, albumin loses approximately 10 percent of its native three-dimensional structure as measured by the alpha helix content in native and transformed forms (25). Increasing the pH to 9 also unfolds the albumin reversibly to an open structure with a 3% change in the alpha helix content. The transition of albumin at higher pH is called N-B transition (28). The three dimensional structure of albumin is also affected by temperature. Stability of albumin is also

temperature dependent. At 37° C, albumin loses 20% of its helical structure. Above 50° C, albumin is denatured irreversibly with a loss of its three dimensional structure.

Most preparations of albumin are heterogeneous in that they contain mercaptoalbumin and non-mercaptopoalbumin. Mercaptoalbumin is the fraction of the albumin with free and reactive sulphydryl groups, responsible for dimerization of the albumin through an oxidation reaction involving the sulphydryl residues. Treatment of albumin with a thiol should break the disulfide linkage of albumin dimer. It has been shown that treatment of albumin with thiol does not necessarily remove all the dimer form (29), however, suggesting that in one type of dimer, the disulfide bond could be located inside the albumin and not exposed to thiols (30). It has also been suggested that hydrogen bonding may be responsible for the stability of the dimer not effected by thiol (30).

Albumin functions as a carrier in the blood transporting water insoluble hormones, steroids like thyroxines and glucocorticoids and free fatty acids. Albumin also transports ions like calcium and zinc.

1.4 Principle of Colloid Stability

The experimental work in this project required stable suspensions of single latex particles. Colloid particles such as polystyrene latex dispersed in an aqueous medium are in constant Brownian motion. These particles are unaggregated only if the potential energy barrier between them is larger than their kinetic energy. The average translational energy of particles in Brownian motion is of the magnitude of $(3/2) kT$ per particle where k is Boltzmann's constant and T is the temperature. Particles are

colloidally stable if the sum of the factors contributing to the potential energy barrier is greater than $2kT$ (31). The net potential energy barrier between colloidal particles is determined by London-van der Waals attraction, electrical double layer repulsion, hydrophobic interaction and excluded volume associated with grafted polymer, if present (32). London-van der Waals forces are short-range dipole-dipole attractive forces caused by the instantaneous charge distribution of polarized molecules. The London- van der Waals free energy of attraction is inversely proportional to the sixth power of the separation distance (31). The total London attractive forces between two particles can be measured by summing all the London forces between molecular pairs (33).

Electrostatic repulsion between the individual ionic double layers also contributes to the stability of colloid particles. In equilibrium, if the surface of a particle is electrically charged, electroneutrality is maintained by arrangement of the counter ions in solution near the particle surface. This surface arrangement is called the electrical double layer (Figure 1.1).

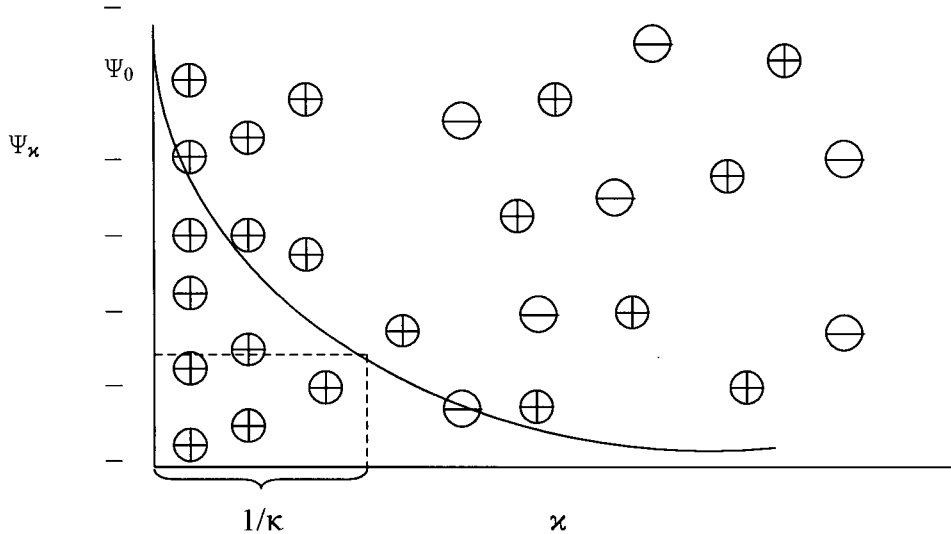


Figure 1.1- Schematic representation of the electrical double layer

For a charged particle, the electrostatic surface potential Ψ_0 decays as a function of the distance from the surface according the following equation:

$$\Psi_x = \Psi_0 \exp[-\kappa x] \quad [1.1]$$

where Ψ_0 = the surface electrostatic potential

Ψ_x = the potential at the distance x from the surface

$1/\kappa$ = electrical double layer thickness

x = distance from the surface of the latex (the surface charge is positioned at the particle- solution boundary, that is, at $x = 0$)

In the absence of polymer, Ψ_x is responsible for the repulsive force between particles, thus responsible for stability of the particles (34). The double layer thickness, $1/\kappa$ is an indicator of the extension of the neutralizing charges from the surface; κ is related to ionic strength of the solution according to the following equations (35):

$$\kappa = [(2000 N_a F^2 I) / (\epsilon_0 \epsilon_r k T)]^{1/2} \quad (m^{-1}) \quad [1.2]$$

$$I = 1/2 \sum c_i z_i^2 \quad [1.3]$$

where N_a = Avagadro number

e = electron charge

I = ionic strength

ϵ_0 = dielectric constant of vacuum

ϵ_r = relative dielectric constant

k = Boltzmann constant

T = absolute temperature

c_i = concentration of ionic species I (moles. dm^{-3})

z_i = valence of i^{th} species

Equations 1.2 and 1.3 imply that the electrical double layer thickness is inversely related to the ion concentration in solution. As electrical double layer thickness, $1/\kappa$ is directly related to Ψ_∞ as shown in equation [1.1], increasing the ion concentration in solution decreases the electrostatic potential and reduces particle stability. According to DLVO (Deryagin-Landau-Verwey-Overbeek) theory for the case where only electrostatic and London-van der Waals interactions are present, a balance of the repulsion between charged particles and London-van der Waals attraction determines the particle stability in a suspension (36).

Another important interaction that contributes to the stability of the particle in suspension is the hydrophobic interaction which produces an attraction force between particles (37, 38). The hydrophobic interaction is due to an increase in the entropy of the solvent. Typically there is excess ordering of the solvent molecules around the hydrophobic surfaces, which is reduced if two hydrophobic surfaces interact. This

increase in entropy of the solvent can be the driving force for particle coagulation.

Another repulsive force which can help stabilize the particles occurs when particles are grafted with a layer of polymer. This repulsion is an entropic effect and is due to loss of configurational entropy of the polymer layers when two particles with adsorbed polymers approach each other to a separation distance less than twice the polymer layer thickness (39). The other important factor for colloidal particle stability is the size of the individual particle. It has been shown that larger particles are more stable than smaller particles (40).

1.5 Interaction of Blood Proteins and Artificial Surfaces

Blood interaction with artificial surfaces is largely governed by the first step of the interaction process which is adsorption of a plasma protein monolayer to the surface. Subsequent platelet and leukocyte adhesion and aggregation, activation of the coagulation cascade, fibrinolysis and in some cases complement activation are controlled by the nature of the layer of adsorbed proteins, that is its composition and conformation (41, 42). For example, it has been shown the absorption of albumin on an artificial surface can reduce platelet activation (43). Conversely, adsorption of proteins like fibrinogen (44, 45), factor XII (46) and von Willebrand Factor (45) enhance platelet activation. Orientation of the proteins on the surface is also important. Antibody dependent activation of the complement system is initiated by the binding of C1q to the F_c regions of groups of IgG; exposure of the F_c region is necessary for complement activation (47).

Adsorption of proteins onto artificial surfaces is a rapid, complex process, variable from surface to surface (48, 49) and variable over time (50, 51). This is particularly true when adsorption is carried out with a mixture of proteins, all capable of interacting with the surface and competing with each other for the interface. The final composition of the protein monolayer is determined by a number of factors including the concentration of the components and their individual affinities for the surface.

1.6 Thermodynamics of Protein Adsorption

Protein adsorption to a surface, at constant pressure and temperature, occurs spontaneously only if:

$$\Delta_{\text{ads}}G = (\Delta_{\text{ads}}H - T\Delta_{\text{ads}}S) < 0 \quad [1.4]$$

where $\Delta_{\text{ads}}G$ = change in Gibbs free energy due to adsorption

$\Delta_{\text{ads}}H$ = change in enthalpy due to adsorption

$\Delta_{\text{ads}}S$ = change in entropy due to adsorption

This means that adsorption occurs when there is favorable interaction between the surface and the protein (enthalpy change) or when there is more disorder in the protein, surface or the solvent (entropy change). Many interactions contribute to the change in enthalpy and entropy during protein adsorption including London-van der Waals, electrostatic, hydrophobic and electrostatic complementarity interactions. The interactions that are major contributors to the process of adsorption are:

1) Hydrophobic interaction of the surface and protein

The main driving force for protein adsorption is due to hydrophobic interaction between the protein and the surface (52). The change in Gibbs free energy due to hydrophobic interaction for a hydrophobic surface as estimated by partition coefficient measurements in water/non-aqueous two-phase systems is -5 to -20 mJ/m² at 25°C (53). This change in the Gibbs free energy by itself is high enough to drive adsorption. The hydrophobic interaction is caused by an increase in entropy of the water molecules surrounding the surface or protein. Generally, there is an excess ordering of the water molecules around the hydrophobic area. Dehydration of the protein or surface increases the entropy by disordering the water molecules and increases protein adsorption. When the protein and surface are both hydrophilic, dehydration of the surface or protein is less favorable and does not promote adsorption of protein to the surface.

2) Electrostatic interaction of the surface and protein

The adsorption of protein can occur through overlapping of the protein and surface electrical double layers. There is a change in the Gibbs free energy when a charged protein is brought close to a charged surface. The amount of the change depends on surface potential and surface charge density. For a protein and surface with opposite charges, the change in the Gibbs free energy is less than zero and favors protein adsorption. The surface charge density changes with each adsorbed protein, therefore the change in the Gibbs free energy is specific for each adsorbed protein. The charge distribution in the electrical double layer is dependent on ionic strength, as

mentioned in Section 1.4, and pH (54), since a change in pH can affect the charge on the protein or surface. Maximum adsorption of the protein occurs at the pH equal to the pI, the isoelectric pH (97). At this pH, the net surface charge of the protein is zero.

3) Structural rearrangements in the protein

The integrity of a protein depends on intermolecular interactions between amino acids as mentioned in Section 1.3. It has been suggested that structural rearrangement, specifically rearrangement of the hydrophobic amino acids in the interior of the protein, may be the driving force for the adsorption of the proteins onto surface (52). It has been shown by transmission circular dichroism, nuclear magnetic resonance and microcalorimetry that a significant portion of a protein's secondary structure can be lost after adsorption (52). If a reactive group that is important for a protein's stability interacts with a surface, conformational changes may result (52). If hydrophobic amino acids in the interior of the protein unfold to interact with a hydrophobic surface, the total Gibbs free energy decreases due to an increase in conformational entropy. This can result in spontaneous adsorption of the protein to the surface.

1.7 Surfaces with a Grafted Hydrophilic Polymer as Biocompatible Surfaces

Based on the different protein-surface interactions, hydrophilic, flexible polymer chains grafted on the surface of a particle should be able to reduce non-specific adsorption of protein for the following reasons:

- a) The hydrophilic nature of the grafted polymer should reduce any driving force that is caused by hydrophobic interaction of the protein and the surface (55-58). The hydrophilic chains also reduce the driving force caused by structural rearrangement of the protein
- b) As protein enters into the hydrophilic grafted chains, the volume available to the grafted chains is decreased. This decrease in configurational entropy is the result of protein moving into the chain exclusion volume and is energetically unfavorable, leading to repulsion (55-58).
- c) If the grafted hydrophilic polymer chain is long enough, it can stretch out beyond the electrical double layer (59). In this case the electrical potential at the outer edge of the grafted chain is negligible and the driving force due to the overlapping of the electrical double layers is minimal.
- d) The chemical potential of the solvent in the grafted chain region is lower than that of the bulk solution, therefore there is a tendency for the solvent to diffuse from the bulk region into the chains. Protein is prevented from adsorbing to the surface due to the repulsion created by the excluded volume of the solvent. This may be the reason that some high water content hydrogels are good biocompatible materials (60).

1.8 Conformation of End-Grafted Chains on a Surface

For a flexible linear polymer in solution, capable of adopting various conformations, the root mean square distance of the segments from the center of the mass R_g can be calculated using random walk statistics (61). The result is (62)

$$\langle R_g^2 \rangle = 1/6 l^2 N \quad [1.5]$$

where R_g = radius of gyration of the polymer

l = segment length

N = number of randomly oriented segment

The calculation for the radius of gyration R_g was improved by deGennes *et al.* (63) who took into account the observation that polymer chains form a more expanded coil in better solvents and by Fleer *et al.* (64) who took into account the facts that polymer chains are not completely flexible due to fixed bond angles (*e.g.*, 109.5° for C-C), that steric repulsion occurs between bulky side groups and that the segments can't overlap each other. The result is

$$\langle R_g^2 \rangle = (b^2/c) l^2 N^\alpha \quad [1.6]$$

where b^2/c is C_∞ , the stiffness parameter which is determined experimentally and α is a constant which accounts for solvent quality and is in the range of $1/2$ in a theta (poor) solvent to $3/5$ in a good solvent.

Based on the radius of gyration of the end-grafted polymers and the distance d between adjacent end-grafted chains ($d \propto \sigma^{1/2}$ where σ = surface coverage (chains/unit area)), two types of conformations for end-grafted chain can be predicted:

a) When the distance between the grafting points is greater than twice the radius of gyration of the polymer chains, a random coil configuration commonly known as a mushroom is adopted (65). For the mushroom configuration, the height of the grafted polymer is independent of surface coverage σ (64) and is given by:

$$h = 2 R_g = 2aDP^{1/2} \quad [1.7]$$

where DP = degree of polymerization

a = constant depending on the nature of the grafted polymer and solvent, Å

If there is favorable interaction between the grafted polymer and the surface, the mushroom can collapse to the surface forming a pancake structure (64)

b) If the distance between grafting points is less than twice the radius of gyration, chain overlap occurs and the chains extend away from the surface due to excluded volume interactions with one another. In this situation, the grafted chains adopt a brush configuration. Chains stretching into the solvent caused by excluded volume of adjacent chains are opposed by the entropic penalty of chain stretching (65-66). In brush configuration, the brush height is related to the length of the chains and surface coverage by following equation (64):

$$h \approx (DP-1)(\sigma l^2)^{1/3} \quad (\text{\AA}) \quad [1.8]$$

where DP = degree of polymerization

l = segment length, Å

σ = surface density

1.9 Theoretical Model to Study Interaction of a Brush Polymer with a Protein

There are many numerical and analytical theoretical models which describe interactions of protein and polymeric surfaces (67-69). The numerical self consistent-field theory is one of the models for the analysis of the interaction of proteins and terminally attached polymers (70). This model is based on an earlier self consistent-

field lattice model of Scheutjens and Fleer (71, 72). The best known use of a lattice model of polymers is due to Flory and Huggins (73-75). They placed the solution in a lattice and used the mean field approximation to find an expression for the change in the free energy of the solution upon mixing solvent with a polymer. Scheutjens and Fleer extended the model to apply to polymer-surface interactions (71, 72). Using the new model, Scheutjens and Fleer developed the self-consistent mean-field theory (SCF) which allowed calculation of the polymer concentration in the direction normal to a surface (z direction). Other investigators improved the SCF model by calculating the density distribution of end grafted chains in one (76) or two dimensions (77).

Based on the SCF theory, Steels *et al.* modeled the interaction of a solute and end-grafted polymer chains (70). They calculated theoretical results for the polymer density distribution of isolated and interacting chains around a solute particle positioned at a fixed distance from the surface and the energy required to move the particle into the polymer chains. They also studied the effect of particle size, chain length, surface density and interaction parameters on density distributions and interaction energies. Some of the most interesting predictions made by their model are for the case where there is an attractive force between end-grafted polymers and the solute. They predict attraction at large distances, changing to repulsion as the solute is moved closer to the surface. Maximum repulsion of the solute occurs on the surfaces with the highest surface density of the grafted polymer. The effect of chain length on the interaction energy was also calculated and is shown in Figure 1.2.

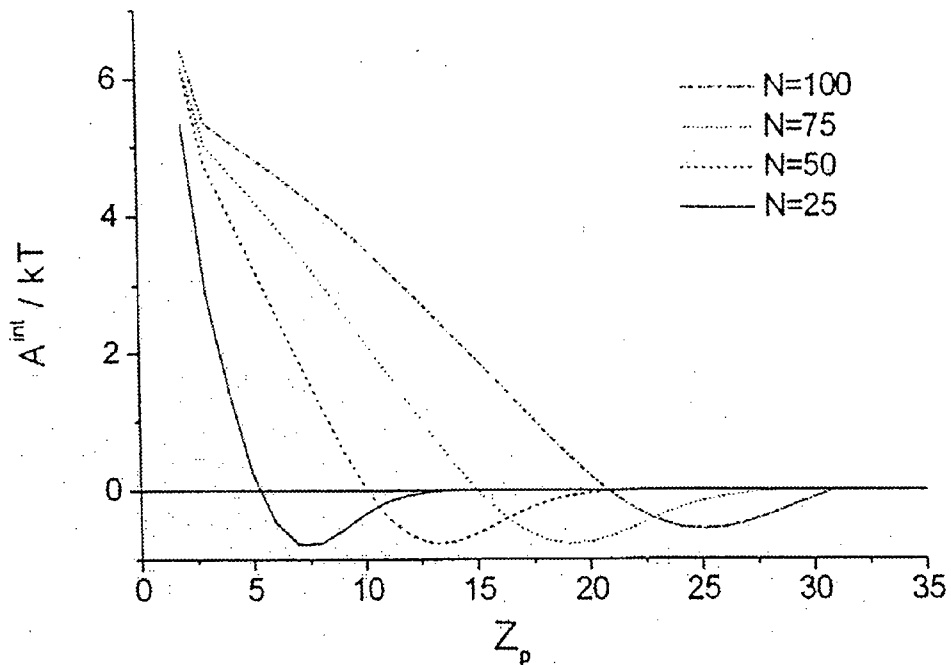


Figure 1.2- Brush-particle interaction energy curves as a function of position Z_p

(lattice layers) are shown for a particle of radius 3 and length 3

(lattice units) penetrating brushes of varied chain length (N), each at

10% grafting density. Interaction parameters are $\chi_{bo} = 0.5$, $\chi_{po} = 0.5$

and $\chi_{bp} = -0.5$ (b= brush, o= solvent and p= particle) (70).

Reproduced by permission of Dr. C. A. Haynes

The repulsion of the solute starts where $A_{int} = 0$ at $Z = Z_{onset}$. For $Z < Z_{onset}$, A^{int} becomes positive. For $Z > Z_{onset}$, A^{int} is negative due to favorable interactions between the solute and the grafted chains. Z_{onset} shifts away from the surface with increasing chain length (N) indicating that the onset of repulsion occurs at greater distances from the surface. Interestingly, longer chains have a broader attractive minimum than shorter chains, resulting in higher probability of adsorption of the solute to the grafted chains.

Based on these results, Steels *et al.* (70) predicted that longer chain lengths may lead to an increase in solute concentration within the polymer chain because for longer chains, more favorable polymer-solute interaction occurs at a similar entropic repulsion.

1.10 Size Exclusion Properties of the Brush Polymer

A new generation of size-exclusion chromatography, entropic interaction chromatography, based on the entropic properties of water-soluble polymer chains has been developed (78). In traditional size-exclusion chromatography (79), the separation of a molecule is thought to be determined by the pore size and the pore volume of the gel particle. The separation occurs as molecules diffuse in and out of the pores of the gel. Smaller molecules have free diffusion into the stationary phase inside the pores and larger molecules are excluded from the stationary phase and remain in the mobile phase (80). Consequently, the molecules are eluted in the order of decreasing size. The partition coefficient (K_d) is defined as:

$$K_d = (V_e - V_o) / (V_t - V_o) \quad [1.9]$$

where V_e = the elution volume of solute molecule

V_t = the bed volume, the total volume available to solute of any size

V_o = the void volume (the elution volume of a very large molecule)

The traditional model of size-exclusion chromatography considers the wall of the pores in the gel matrix to be rigid with no interaction occurring between the solute and the gel. Brooks and Müller (78) proposed an alternative model, considering both enthalpic and entropic interactions between the solute and the gel matrix. Using the

mean-field theory of Flory and Huggins (62), the partition coefficient of a macromolecule between a solvent and polymer (the gel is treated as a macromolecule solution of finite or infinite molecular weight polymer) is predicted in the first order expression 1.11:

$$K = \Phi_{3,P} / \Phi_{3,S} \quad [1.10]$$

$$K = \exp(-P_3\Phi_{2,P}\{(1-1/P_2)-(\chi_{13}-\chi_{23})\}) \quad [1.11]$$

where Φ_i = volume fraction of polymer i (\propto concentration)

P_i = volume of polymer i / volume of solvent (\propto molecular weight)

χ_{ij} = Flory interaction parameter (\propto chemical interaction)

1 = solvent

2 = polymer

3 = macromolecular solute being partitioned

s = solvent phase

p = polymer phase

The Flory interaction parameter is defined as:

$$\chi_{ij} = Z\Delta\epsilon_{ij} / kT \quad [1.12]$$

where Z = number of contacts per polymer segment

$$\Delta\epsilon_{ij} = \epsilon_{ij} - \frac{1}{2}(\epsilon_{ii} + \epsilon_{jj})$$

$\Delta\epsilon_{ij}$ = the difference in interaction energy between polymer-solvent (ϵ_{ij}),

polymer-polymer (ϵ_{ii}) and solvent-solvent (ϵ_{jj}) contacts.

k = Boltzmann constant

T = temperature

Expression 1.11 predicts that the log of the partition coefficient of a macromolecular solute into a polymer solution (the ratio of the concentration of the macromolecular solute in the polymer and solvent) is proportional to the solute molecular weight P_3 and polymer concentration $\Phi_{2,P}$ (\propto 1/porosity of the gel) and inversely to gel polymer molecular weight P_2 . The partition coefficient is also related to the difference in enthalpic interaction of the macromolecular solute with the solvent and polymer ($\chi_{13}-\chi_{23}$). Based on the above expression, the partition of the solute into the brush polymer is predicted for the case where there is no solute-polymers or solute-solvent interaction ($\chi_{13} = \chi_{23} = 0$). This partition is inversely related to the solute molecular weight, polymer brush length (\propto polymer molecular weight) and polymer brush grafting density (\propto polymer concentration). The model was supported by showing that size-based separation could be achieved using entropic interaction chromatography (78, 81).

CHAPTER 2

Polystyrene Latex Synthesis and Grafting of Poly(2-methoxyethylacrylate) and Poly(N,N-dimethylacrylamide)

2.1 Polystyrene Latex Synthesis

2.1.1 Materials

Styrene monomer, ACS grade, was obtained either from Fisher (Fair Lawn, NJ) or Aldrich (Milwaukee, WI), and was distilled under reduced pressure at 40°C and stored under argon at -70°C before usage. Acrolein was from Aldrich and was distilled at 56°C under argon atmosphere before storage at -70°C in the dark. 2,2'-Azobis(2-amidinopropane) dihydrochloride (ABA.2HCl) was purchased from Wako Pure Chemical Industries Ltd. (Osaka, Japan) and was used without further purification. Sodium bromide ACS grade was from Fisher and was used without further purification. Standard HCl and NaCl solutions used for titrations were from Fisher. Hydroxylamine hydrochloride (99% purity) was purchased from Aldrich and used for titration. Distilled water was further purified by a Milli-Q plus water purification system.

2.1.2 Synthesis Method

2.1.2.1 Synthesis of Latex Seed

Surfactant-free polystyrene latex seeds, FS1, FS2, FS3 and FS4 were synthesized according to the method by J.W.Goodwin (82). Distilled water (620 ml) and 0.872 g of NaBr were added to a three-necked flask (1 L capacity) equipped with an overhead stirrer and a condenser and immersed in a thermostated water bath. The flask was filled and evacuated with argon eight times while stirring at the rate of 350 rpm at room temperature. The temperature was increased to 70°C and 34.71 g of styrene was added under slow argon flow. After five minutes, 0.54 g of the initiator, ABA.2HCl, dissolved in 100 ml distilled water was added. The reaction was allowed to proceed at 70°C for 24 hours under slow argon flow stirring at 350 rpm. The latex was filtered through glass wool to remove aggregates before dialyzing against water for one week in a 40 L tank with daily water changes. The latex was then washed three times with distilled water by centrifugation and supernatant replacement before storage in polyethylene containers at 4°C. Two weighed aliquots of the latex suspension were freeze-dried to determine solid content.

2.1.2.2 Seeded Polymerization

Seeded polymerization was carried out according to Hritcu *et al.* (81) to obtain monodisperse polystyrene latex in the size range of 2-3 μm suitable for chromatography. Three steps seeded polymerization were carried out to produce latexes FP1, FS4P (first step), FP2, FS4P2 (second step) and FP3, FS4P2P' (third

step). The procedure for seed polymerization was as follows: the polystyrene seed (final solid concentration 3.15%) was weighed into a three-necked flask (0.5 litre capacity) and filled and evacuated eighth times with argon while stirring at 350 rpm at room temperature. The temperature was increased to 50°C before styrene (80 g/L) was added under argon. The argon flow was adjusted to one or two bubbles per second. After five minutes, the initiator, ABA-2HCl (4.4×10^{-3} moles/L) was added under argon. The latex was collected and filtered through glass wool to remove aggregates before dialyzing against water for one week in a 40 L tank with daily water changes. The latex was then washed three times with distilled water by centrifugation and supernatant replacement before storage in polyethylene containers at 4°C. Two weighed aliquots of the latex suspension were freeze-dried to determine solid content.

2.1.2.3 Acrolein /Styrene Copolymer Shell

Seeded growth copolymerization of styrene and acrolein was carried out according to Hritcu *et al.* to synthesize latexes: FS2A, FS2A2, FS3A and FS4P2P'A (81). The purpose of the seeded growth copolymerization was to introduce aldehyde groups on the surface of latex. These aldehyde groups were the reducing agents to which the polymer is grafted. For this purpose, surfactant-free polystyrene seeds (final solid concentration 3.3%) were charged inside a three-necked flask (0.5 L capacity) and filled-evacuated eighth times with argon while stirring at 350 rpm at room temperature. The temperature was raised to 50°C and styrene (2×10^{-3} moles/g of seeds) added under argon and the mixture was allowed to equilibrate for 15 minutes. Acrolein (2×10^{-3} moles/g of seeds), dissolved in 10 ml deionized water, was added

and allowed to equilibrate for 5 minutes. The initiator, ABA-2HCl (9.2×10^{-4} moles/L) was then added and the reaction was allowed to continue for 6 hours. The latex was filtered through glass wool to remove aggregates before dialyzing against water for one week in a 40 L tank with daily water changes. The latex was then washed three times with distilled water by centrifugation and supernatant replacement before storage in polyethylene containers at 4°C . Two weighed aliquots of the latex suspension were freeze-dried to determine solid content.

2.1.3 Analytical Methods

2.1.3.1 Size Distribution of Latex

Latex size distribution was measured using a scanning electron microscope (SEM). A $20 \mu\text{l}$ aliquot of latex suspension was dried onto a carbon disk and coated with gold particles under vacuum. A minimum of 100 latex particles was randomly analyzed with an image analysis program (Image Tool, University of Texas, Houston) to determine the distribution and average size of the latex population.

2.1.3.2 Surface Charge Density

Latex seeds and seeds with an acrolein shell are stable in aqueous media due to the presence of positively charged amidine groups on the surface derived from the initiator (ABA-2HCl), according to following reaction:

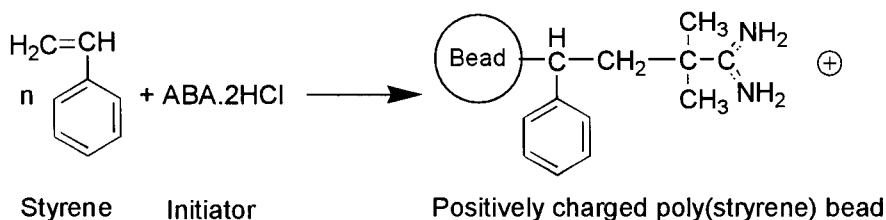
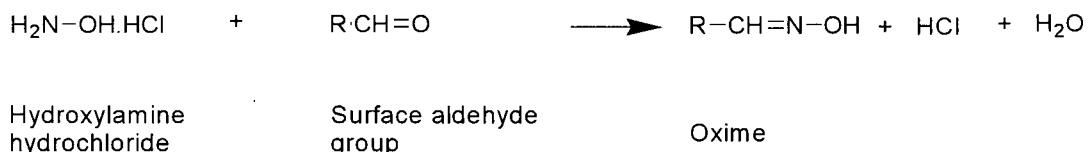


Figure 2.1- Positively charged poly(styrene) latex

The surface charge density of the latex was measured by a conductometric titration technique (83). The latex was washed twice with deionized water and transferred into a polypropylene container. Two weighed aliquots were removed from the latex suspension and freeze-dried to determine solid content. The latex suspension was degassed with argon before a minimum of 0.5 g of latex in 10 ml deionized water was transferred into the conductometric cell. The conductometric cell was kept under slow argon flow with vigorous stirring. A precision syringe pump (Harvard Apparatus, Infusion/Withdrawal pump, model 9322, South Natick, MA) was used to deliver 0.0100 M titrant (HCL) into the cell at a constant flow rate while a conductivity meter (YSI Scientific Model 35, Yellow Springs, OH) measured conductance. The equivalence point was determined from the plot of conductance *versus* volume (ml) of titrant. A back titration was done with NaOH (0.0100 M) to obtain a second value for the equivalence point. The average of the two values was used to calculate the surface charge per unit weight. From the latex size as measured by SEM and the density of bulk polystyrene (1.0525 g/cm³), the surface area and the surface charge density were calculated.

2 .1.3.3 Aldehyde Content of Copolymer Shell

The aldehyde content of the copolymer shell was measured by conductometric titration as described by Yan *et al.* (84). A latex suspension with styrene-acrolein copolymer shell was mixed with a 0.1 M solution of hydroxylamine in a glass vial and the reaction was allowed to continue overnight while tumbling on a rotating rack. The aldehyde groups on the surface of the latex react with hydroxylamine according to the following reaction:



The hydrochloric acid produced in this reaction was titrated twice conductometrically with standard sodium hydroxide as described in section 2.1.3.2. The aldehyde content of the sample was calculated with the following formula:

$$\text{Group/Area (charged groups}/\text{\AA}^2) = (\text{NFDR} \times 10^{-16}) / 3$$

N = Avogadro's constant

F = moles of aldehyde per gram of latex (titration graph)

D = density of polystyrene (1.0525 g/cm³)

R = radius of the latex (cm)

2.1.3.4 Electrophoretic Mobility

Electrophoretic mobility was measured in a microelectrophoresis apparatus with a cylindrical chamber (Rank Mark I, Rank Bros, Bottisham, UK) with a Ag/AgCl reversible electrode system as described by Seaman (85). The rate of migration of a minimum of 10 latex particles suspended in 100 mM NaCl of different pH values toward both positive and negative electrodes was measured at the stationary level as they moved across the eyepiece reticule at 25⁰C. The electrophoretic mobility, μ , was calculated from the averaged velocities, v, the applied voltage, V, and the chamber electrical length, l_E according to the following equation:

$$\mu = v \cdot l_E / V \quad [2.1]$$

2.1.4 Results

Three batches of latex were prepared for grafting. The characterization of the latex at each stage of the polymerization is in Table 2.1.

Latex	Radius (μm)	Charged groups or aldehyde groups (for latex designated A) per gram of latex (moles/g)	Surface area per charged group ($\text{\AA}^2/\text{moles}$)	Surface area per aldehyde group ($\text{\AA}^2/\text{moles}$)
FS1	0.41 ± 0.07	2.94×10^{-6}	393	-
FP1	0.59 ± 0.1	3.44×10^{-6}	235	-
FP2	0.8 ± 0.2	2.69×10^{-6}	220	-
FP3	1.33 ± 0.3	1.85×10^{-6}	192	-
FS2	0.45 ± 0.06	N.D.*	N.D.*	-
FS2A	0.45 ± 0.06	1.09×10^{-5}	-	70
FS3	0.395 ± 0.1	4.52×10^{-6}	265	-
FS3A	0.395 ± 0.1	2.47×10^{-5}	-	49
FS4	0.45 ± 0.1	3.61×10^{-6}	292	-
FS4P	0.7 ± 0.1	2.06×10^{-6}	328	-
FS4P2	1.25 ± 0.2	2.36×10^{-6}	157	-
FS4P2P'	1.78 ± 0.3	1.16×10^{-6}	229	-
FS4P2P'A	1.78 ± 0.3	3.4×10^{-6}	-	79

* - N.D.- not determined

Table 2.1- Characterization of the seed latexes with or without acrolein shells.

Uncertainties in these values are discussed at the end of section 2.1.5.

Legends are discussed in section 2.1.2

2.1.5 Discussion

Polystyrene by itself has no application as a biomaterial because it tends to adsorb proteins strongly by hydrophobic interactions. However, it has been reported that polystyrene in conjunction with another polymer can be useful as a biomaterial (86). For example, polystyrene and a hydrophilic polymer poly(2-hydroxyethylacrylamide) (HEMA) can form a hydrophobic-hydrophilic block. Upon exposure of the hydrophobic-hydrophilic block to a hydrophobic surface, the hydrophobic portion of the block (polystyrene) is adsorbed via hydrophobic interactions and hydrophilic areas orient toward the aqueous solution. As a result, the extended hydrophilic polymer rejects protein (87). Polystyrene latex covered with a covalently bound dense tethered polymer provides a useful system in which to study biocompatibility because they provide a large surface allowing chemical determination of surface groups to be carried out. Latex FP3 and FS4P2P'A were prepared for chromatography. Latexes with a minimum diameter of 2.5 microns are desirable for this application since smaller latex can create high back pressure in the column. It has been reported that three consecutive seeded polymerizations will produce a latex with diameter of approximately 2.5 μm (89). FP3 had an average diameter of 2.66 μm after three seeded polymerizations. In comparison, FS4P2 had a diameter of 2.56 μm after only two seeded polymerizations. A third seeded polymerization of FS4P2 increased the size to 3.56 μm (FS4P2P').

Several theories have been suggested for the growth of latex particles by seeded polymerization, including the heterocoagulation theory (88). This theory, which seems to be reasonably well accepted, suggests that in general freshly formed particles,

swollen with monomer, transfer monomer to the seed particle by coagulation (90). When the initiator is added to the aqueous phase, new primary particles are formed. Three possible coagulation processes involving these primary particles can then occur. First, primary particles can homocoagulate. In the absence of the seed particles, this is the most important reaction since newly formed particles, being small, of low surface density and swollen with monomer are not stable. Second, the primary particles can heterocoagulate with the seed particles to gain stability. The monodispersity of the final product depends on these two coagulations. In the presence of high concentration of the seed particles, heterocoagulation of the seed with new primary particles is preferred and a reasonably monodisperse product is obtained. Conversely, if the initial concentration of the seed is not high enough, homocoagulation of the new primary particles can occur which along with heterocoagulation produces a bimodal final product.

Finally, the seed particles can coagulate with each other. This is unlikely to occur because the seed particles are very stable due to their large size and positive surface charge. However, if they do become unstable, they can homocoagulate and produce a large particle. Homocoagulation of seeds may have occurred during the second seeded polymerization of batch FS4-FS4P2P'A. During this step, seed FS4P volume grew by almost a factor of 6 ± 2 . It is interesting to note that no aggregation of the latex was observed during this step and a very high yield was obtained. Knowing the density of the polystyrene, the size of the latex and the total yield, the total number of seed particles before and after the reaction were calculated to be $(7 \pm 3) \times 10^{12}$ particles and $(2 \pm 1) \times 10^{12}$ respectively.

The presence of a polymerization inhibitor in the reaction mixture could be responsible for seed homocoagulation of batch FS4-FS4P2P'A. If the inhibitor in styrene monomer was not completely removed by distillation, it could reduce the formation of the new particles in the bulk solution. It has been shown that monomers under typical polymerization conditions are absorbed inside the latex particles, although the diffusion flux of the monomer into the latex is small (88). In the absence of primary particle formation, monomer diffuses into the seed and causes swelling. If initiator also diffuses to the surface of the seed, polymerization of monomer associated with the seed can occur. Polymerization in the seed particles continues until they become unstable due to lower surface charge density. Eventually, two unstable seeds coagulate to gain stability.

FS2A and FS3A with a diameter of approximately 0.8 μm and a specific surface area of $7.2 \times 10^4 \text{ cm}^2/\text{g}$ were prepared to study albumin adsorption to the grafted polymers based on 2-methoxyethylacrylate and N,N-dimethyl acrylamide.

The biggest uncertainty associated with the values of aldehyde or charge group concentration (Table 2.1) is from error associated with reading of the equivalence volume from the conductometric titration curve. Considering a maximum error of $5 \times 10^{-3} \text{ ml}$ in reading the volume, the concentration of the titrant (0.1 M) and the average weight of the sample (0.5 g), the uncertainty was calculated to be 5 to 25% of the measured aldehyde or charge concentration. However as the value of the aldehye or charge concentration was the average of two measurements and the difference between two was not more than 3 to 6 %, it is reasonable to assume maximum of 10% in uncertainty.

2.1.6 Conclusion

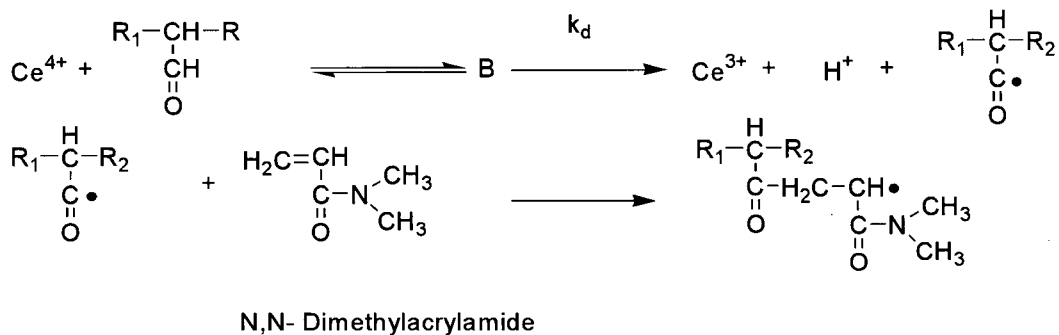
Four latexes were prepared for use in the adsorption and chromatography experiments. FP4 coagulated during core-shell copolymerization and could not be used. Seeds FS2A2 and FS3A were coated with poly(styrene-co-acrolein) shell and used in the adsorption experiments. To produce latex FS4P2P'A for chromatography, the seed, FS4, was grown three times via seed-polymerization before introduction of the poly(styrene-co-acrolein) shell.

2.2 Ce(IV) Initiated Graft Polymerization

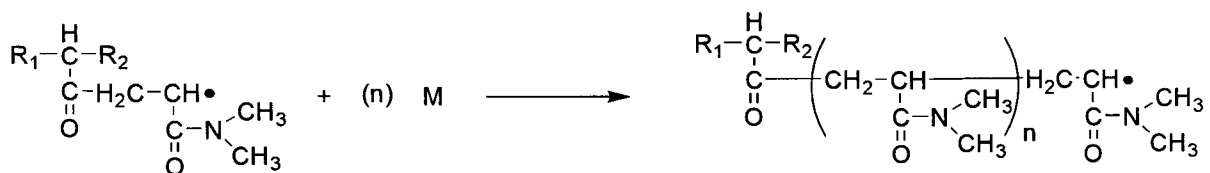
2.2.1 Introduction

The Ce(IV) redox system was used for the synthesis of the grafted polymer. The advantage of using ceric salts for graft polymerization is in the simplicity of use, the high grafting efficiencies obtained and the relative lack of solution polymerization in appropriate systems (89-91). The mechanism of Ce (IV) initiated polymerization is shown in Figure 2.2, where M refers to a molecule of monomer.

1. Initiation



2. Propagation



3. Termination

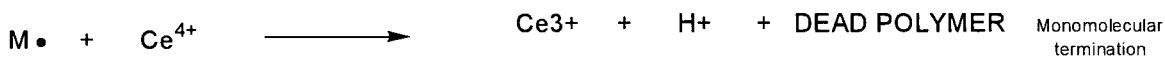


Figure 2.2- Mechanism of Ce (IV) initiated graft polymerization

It has been shown that the rate limiting step in this mechanism is k_d , the rate of dissociation of B, the complex formed between the reducing agent (in this case aldehyde on the surface) and Ce (IV) (91). The efficiency of Ce (IV) initiated grafting is dependent on the concentration of monomer, cerium concentration and acid in the reaction mixture (91, 92). Reaction time and temperature also contribute to the grafting efficiency (96). The monomers, 2-methoxyethylacrylate and N,N-dimethylacrylamide, were grafted using the Ce (IV) redox system.

2.2.2 Materials

Cerium(IV) ammonium nitrate ($(\text{NH}_4)_2\text{Ce}(\text{NO}_3)_6$), (99.99% purity), ethylenediaminetetraacetic acid trisodium salt hydrate (EDTA), 2-methoxyethylacrylate (MEA) and N,N-dimethylacrylamide (DMA) were purchased from Aldrich. The inhibitor was removed by fractional distillation under vacuum. The concentrated acetic acid and nitric acid were purchased from Fisher. A 50x10 mm Superformance column (E.Merck, Darmstadt) packed with Merck Licospher RP 60-Select B beads (E.Merck) was used to determine the amount of unreacted monomer during grafting by HPLC analysis (performed on a Merck-Hitachi Iner Version system, E.Merck; Monitor L4200, Merck-Hitachi).

2.2.3 Methods

The method used for Ce (IV) initiated grafting polymerization was that of Hritcu (89) and Müller (90) with a minor adaptation when grafting experiments were carried out in test tubes. Known amounts of latex and monomer were added to a reaction vessel or a test tube, degassed and flushed with argon three times. The appropriate amount of cerium (IV) ammonium nitrate in 10 mM nitric acid solution was degassed and added through a rubber septum with a syringe. The reaction mixture was swirled well to mix and placed in a water bath at 40° C for one hour with stirring. After one hour, the water bath was cooled to room temperature. The reaction was allowed to continue under slow argon flow and slow stirring. Samples were taken from the reaction mixture throughout the grafting experiment and passed through a 0.2 μm low protein binding filter (Gelman Sciences, Ann Arbor, MI). The supernatant was

collected and evaluated for monomer content by reverse phase chromatography (RP60). When the reaction was complete, the latex was centrifuged and the supernatant removed and evaluated for monomer content. The latex was then washed three times with distilled water; once with 0.1 ml sodium sulfite solution in 0.1 M acetic acid to convert residual Ce (IV) to Ce (III) and once with 0.03 M EDTA to remove Ce (III). The latex was washed three more times with distilled water before storage in a polyethylene container at 4° C. Nitrogen analysis of the grafted and non-grafted latex was performed by SGS Canada Inc, Vancouver, BC.

2.2.4 Results:

2.2.4.1 Ce(IV) Initiated Grafted Polymerization of 2-methoxyethylacrylate(MEA)

Grafting with 2-methoxyethylacrylate (MEA) was unsuccessful due to a high degree of solution polymerization. The reaction mixture became very viscous within 2 minutes after the addition of the Ce(IV), aggregating the latex and stopping the stirring. This suggests that the rate of polymerization of the MEA in solution was faster than the rate of the reaction of cerium ion with reducing aldehyde groups on the latex surface. Two possible mechanisms could contribute to the higher rate of polymerization of MEA in solution

a) 2-methoxyethanol may have been produced by the hydrolysis of the monomer in an acidic medium according to following reaction:

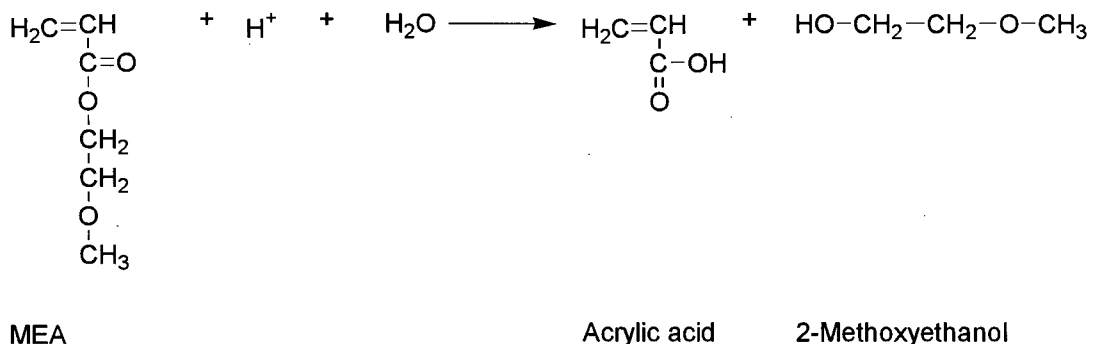


Figure 2.3- Hydrolysis of the 2-methoxyethylacrylate in an acidic medium

The 2-methoxyethanol can act as reducing agent and initiate solution polymerization. If this was the case, the other product of this reaction, acrylic acid should increase the hydrogen ion concentration in the solution. A conductometric titration on the supernatant of the reaction mixture determined that the concentration of the H^+ was in fact decreased by a factor of 1.3, however.

b) The ceric ion can initiate spontaneous homopolymerization of vinyl compounds such as acrylamide in solution. In the case of acrylamide the rate of homopolymerization is much slower than the rate of the reaction between the cerium ion and the reducing agent, therefore the ceric ion initiated graft polymerization of acrylamide occurs without significant competing spontaneous homopolymerization in solution (93). If the rate of spontaneous homopolymerization of MEA in solution is faster than the rate of reaction between the cerium and the reducing agent, lowering this rate should promote cerium initiated grafting of the latex.

To examine this, two separate sets of experiments were conducted. In the first, the concentration of latex, monomer, and cerium ion were varied and the effect on

increased solution viscosity and stirring was recorded (Table 2.2). In all reactions stirring stopped within two minutes after addition of the cerium ion, indicating that the solution polymerization rate was not dramatically affected by reactant concentrations. In the second set of experiments, different concentrations of a retarder, phenothiazine, were added to the monomer without latex and the effect on the increase in solution viscosity and stirring was recorded. Phenothiazine slows down the polymerization process by competing for radicals. None of the reactions with retarder stopped after 10 minutes, however eventually the stirring stopped due to a large increase in viscosity (Table 2.3). The higher the concentrations of the phenothiazine, the longer the reaction continued. But since high concentration of the retarder in the reaction mixture can affect both solution and graft polymerization of the MEA, it was felt that addition of the retarder was unlikely to promote graft polymerization in the presence of solution polymerization.

Latex	[Mon]/[Ald]	[Ini]/[Ald]	Observation
FS1A	609	34	Aggregated(<2 min)
FS2A	675	33	Aggregated(<2 min)
FS2A	672	101	Aggregated(<2 min)
FS2A	535	31	Aggregated(<2 min)
FS2A	360	21	Aggregated(<2 min)
FS2A	326	11	Aggregated(<2 min)
FS2A	202	48	Aggregated(<2 min)
FS2A2	285	4	Aggregated(<2 min)
FS2A2	16	6	Aggregated(<2 min)

[Mon] = Monomer concentration (M)

[Ald] = Aldehyde on latex surface per unit volume (M)

[Ini] = Initiator concentration (M)

Table 2.2- Ce (IV) initiated grafting of the 2-methoxyethylacrylate at different concentration of monomer, aldehyde and initiator

Latex	[Ini]/[Mon]	[Ret]/[Mon]	Observation
FS2A2	.079	1.53E-2	Aggregated(~10 min)
FS2A2	0.072	3.37E-2	Aggregated(~13 min)
FS2A2	0.074	5.7E-2	Aggregated(~14 min)
FS2A2	0.076	1.58E-1	Aggregated(~17 min)
FS2A2	0.074	1.20	Aggregated(~30 min)
FS2A2	0.078	1.27*	Aggregated(~30 min)

* Inhibitor was dissolved in 0.5 gram toluene

[Mon] = Monomer concentration (M)

[Ret] = Retarder concentration (M)

[Ini] = Initiator concentration (M)

Table 2.3- Ce (IV) initiated grafting of the 2-methoxyethylacrylate at different concentration of monomer, retarder (phenothiazine) and initiator

2.2.4.2 Ce (IV) Initiated Grafted Polymerization of N,N-dimethylacrylamide

Ce (IV) initiated graft polymerization of N,N-dimethylacrylamide (DMA) onto the latex was also carried out with the results shown in Table 2.4. The reaction mixture viscosity did not obviously increase throughout the grafting reaction indicating minimal solution polymerization. The grafting efficiency for this monomer was very high and an average of 80% of the monomer was consumed in the reaction after 20 hours.

Batch #	Chain Separation (Å)	DP		Radius of gyration (Å)		Brush height (Å)	
		HPLC	N ₂	HPLC	N ₂	HPLC	N ₂
FS3AG	7	207	154	37	32	70	52
FS3AG2	7	116	18	28	11	39	6
FS3AG3	7	560	220	61	39	191	75
FS4P2P'AG	9	1310	NA	94	NA	382	NA

Table 2.4- Characterization of the polystyrene latexes grafted with N,N-dimethylacrylamide

The latex, FS3A was grafted with three chain lengths of poly(N,N-dimethylacrylamide) (FS3AG, FS3AG2 and FS3AG3) and was used in protein adsorption experiments. The latex, FS4P2P'A was grafted with one chain length of poly(N,N-dimethylacrylamide) (FS4P2P'AG) and was used for both protein adsorption and size exclusion chromatography experiments. Electrophoretic mobility measurements of the latex before and after grafting were plotted versus pH and the results are shown in Figures 2.4 and 2.5.

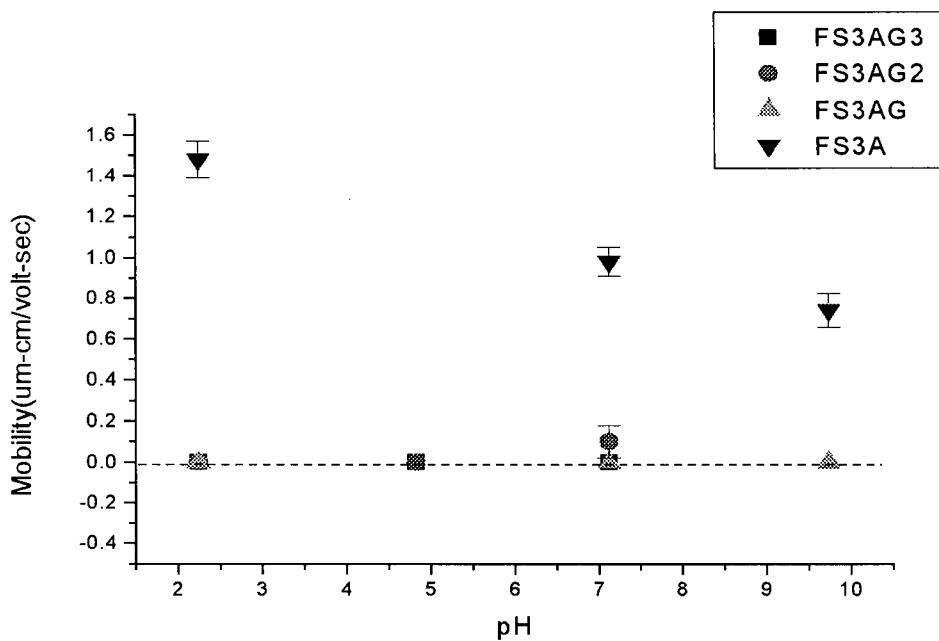


Figure 2.4- Microelectrophoretic mobility measurement of the polystyrene latex (diameter = 0.79 μm) before (FS3A) and after the grafting (FS3AG, FS3AG2, FS3AG3) with N,N-dimethylacrylamide (N = 10, Error bars are \pm one standard deviation).

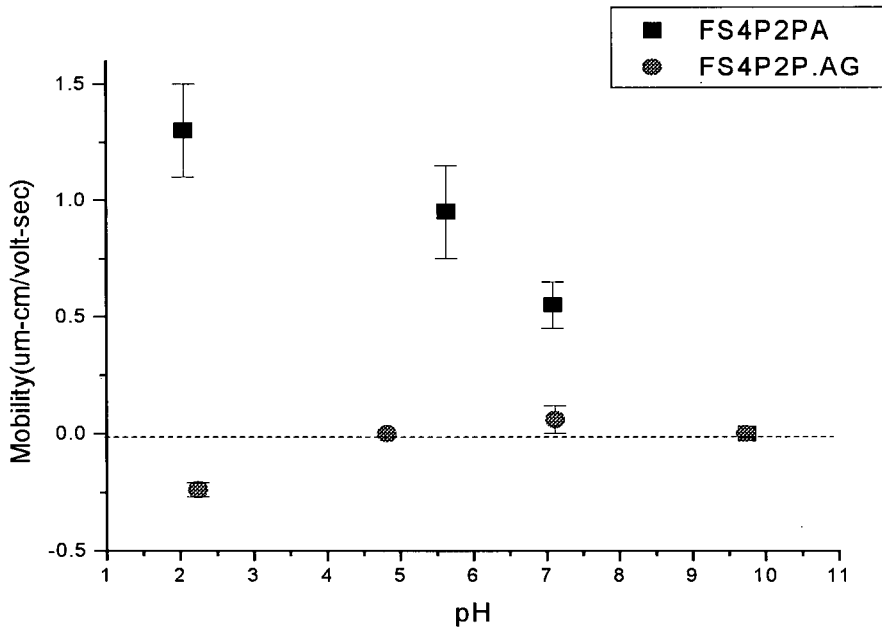


Figure 2.5- Microelectrophoretic mobility measurement of the polystyrene latex (diameter = 3.55 μm) before (FS4p2p'A) and after the grafting (FS4P2P'AG) with N,N-dimethylacrylamide (N = 10, Error bars are \pm one standard deviation).

2.2.5 Discussion

The positive charge on the latex is derived from initiator residues as shown in Figure 2.1. The pH-dependency of the charged latex depends on the pKa of the amine groups of the initiator. At lower pH, the amine groups are protonated and retain a positive charge. At the pH values above the pKa, amine residues lose one hydrogen and become neutral.

The electrophoretic mobility of the grafted latex decreased to virtually zero at each pH. The grafted polymer extends into solution so far beyond the positive surface charge that the electrophoretic potential at the outer edge of the grafted layer is essentially zero, causing the very low mobilities observed (59). Electrophoretic mobility measurements of the polystyrene latex grafted with 2-methoxyethylarylamide were carried out by Hritcu *et al.* (81). The positive polystyrene latex retained a positive mobility after the grafting because short grafted poly(2-methoxyethylacrylamide) did not extend beyond the electrical double layer.

Three different chain lengths of the poly(N,N-dimethylacrylamide) were grafted on latex FS3A by varying the amount of monomer in the reaction mixture. Higher concentrations of monomer increase the length of the grafted polymer through mass action as shown previously (92, 94).

The degree of polymerization of the grafted polymers *DP* (Table 2.4) was calculated by two methods: HPLC and nitrogen analysis

A) HPLC

The amount of monomer consumed was determined by analyzing the monomer content of the supernatant at the end of the reaction using HPLC with a reverse phase column (RP60). The monomer content was determined from a monomer concentration vs peak area calibration curve and used to calculate the degree of polymerization.

B) Nitrogen Analysis

Weighed aliquots of the grafted latex were freeze-dried and nitrogen content was determined by combustion. A sample of non-grafted latex was also analyzed for nitrogen content for comparison.

In both analyses, it was assumed that graft polymerization was initiated on every aldehyde group on the latex surface and that all grafted chains were terminated at the same point so that all brush heights were equal. For HPLC analysis calculation, it was further assumed that all the monomers were incorporated into the grafted polymer and no solution polymerization occurred.

By ignoring solution polymerization, the values obtained for the DP by HPLC analysis were likely overestimated. As shown in Table 2.4, the DP values calculated from nitrogen analysis were lower than those obtained from HPLC analysis. There was a large uncertainty associated with the DP values determined from nitrogen analysis due to the large size of the latex, relatively small surface area per gram of latex and the small amount of the grafted DMA. In fact the nitrogen content was near the limit of detection of the method (Appendix, Table A.1). Ignoring this, the difference between two analyses, before and after the grafting, should determine the degree of solution polymerization. These corresponds to 26%, 84% and 60% of the total DMA polymerized for grafted latexes FS3AG, FS3AG2 and FS3AG3, respectively. The

values for degree of solution polymerization of DMA implied do not support the small viscosity increase during the reaction, however. Both analysis methods showed the same trends for DP of grafted polymer on the latex. For each grafted latex, chain separation, radius of gyration and brush height was calculated using both methods. A sample calculation can be found in the Appendix. Chain separation of the grafted polymer was calculated using values of aldehyde concentrations found by conductometric titration of the latex. The uncertainty associated with chain separation values is the same as for the aldehyde concentration values (10%). The error associated with the DP values measured by nitrogen analysis was not calculated as there was no error reported by SGS Canada Inc. The largest error associated with the DP values measured with HPLC was due to measuring the concentration of the monomer at the end of the reaction. Considering a 40% error in measuring this concentration, a 10% error is associated with DP values. For one sample, the monomer content was measured twice. The error associated with the DP value due to the difference in monomer content of this sample was 5%. Therefore, it can be assumed that the DP value error for HPLC analysis is 5 to 10%.

From the data in Table 2.4, assuming equal length chains grew from each aldehyde implies that for all latexes, the grafted chains were of brush configuration because the values for the radius of gyration were larger than those for chain separation.

There is also potentially an error associated with the DP and chain separation values due to the assumption that grafting was initiated from every aldehyde group on the surface. If grafting was not initiated from all aldehyde groups, both chain

separation and DP values would increase. Assuming grafting initiated on 75% of the aldehyde groups, there will be a 10 % error increase in the DP and R_g values. The assumption does not have an impact on the conclusion of a brush configuration for the grafted polymer, therefore.

There is also the possibility of having non-equal chain lengths. Hritcu *et al.* (89) have shown that for poly(2-methoxyethylacrylamide) grafted polymers on polystyrene latex bearing functional hydroxyl groups, two categories of the terminally attached grafted chains are possible: a long polymeric grafted chain and a short polymeric grafted chain. They reasoned that the distribution of the size in the grafted chain depends on the local density of the functional hydroxyl groups. For those areas of the surface with high local density of the hydroxyl groups, chains are sufficiently close to each other to mutually terminate by combination or disproportionation. These grafted polymers account for the short grafted chain population. For surface regions with lower density of the hydroxyl groups, the chains continue to grow and form the long grafted chain population. The long grafted chains can also restrict monomer diffusion towards shorter growing chains located under them which could result in bimodal populations of the chains. In bimodal populations of the grafted chains, the shorter chains and the longer chains, depending on surface coverage, can have brush or mushroom configuration.

2.2.6 Conclusion

Grafting of 2-methoxyethyl acrylate and N,N-dimethylacrylamide was attempted on latex carrying functional aldehyde groups. Grafting of 2-

methoxyethylacrylate to the latex was not successful due to the high rate of solution polymerization of the monomer. The grafting efficiency of N,N-dimethylacrylamide to latex FS3A and FS4P2P'A was very high with no significant increase in the viscosity of the reaction mixture. Particle microelectrophoresis measurements on the grafted latex indicated that a relatively dense layer of neutral chains was present external to the charged surface, reducing the mobility to nearly zero. The chains grafted on latex FS3A and FS4P2P'A were likely of a brush configuration.

CHAPTER 3: Adsorption of Human Serum Albumin on The Grafted Latex

3.1 Adsorption Isotherm

3.1.1 Introduction

Human serum albumin (HSA) is the most abundant protein in blood, being present at a concentration of about 46.2 ± 2.9 g/L in serum. HSA binding to biocompatible materials has been investigated extensively because HSA is one of the first proteins to bind to the surface (95). Radioactively labeled HSA adsorption to latex covered with tethered poly(N,N-dimethylacrylamide) was used to study the effect of tethered chains on protein adsorption. Radioactive labeling with ^{125}I is the method of choice to measure protein concentration in an adsorption experiment because of its high sensitivity and accuracy. ^{125}I labeled HSA was added to the grafted latex and the adsorption was monitored by depletion and directly by measuring the amount of radioactivity of the latex pellet following buffer washing. To compensate for the small amount of latex lost during washing, the amount of adsorbed HSA was measured in microhematocrit tubes in which the amount of latex counted could be determined.

3.1.2 Materials

Human serum albumin lot # 32H9300 (MW= 66000, isoelectric point 4.71) was purchased from Sigma, Mono and dibasic sodium phosphate were purchased from Sigma (St. Louis, MO). Iodo-beads were purchased from Pierce (Rockford, IL). Na^{125}I with an initial specific activity of 618 MBq per μg of iodide was purchased from

Amersham Pharmacia Biotech (Quebec, Canada). Size exclusion resin (Sephadex-25 medium) was from Pharmacia (Uppsala, Sweden). Microhematocrit capillary tubes and trichloroacetic acid were purchased from Fisher. Sodium dodecyl sulfate was from Biorad (Richmond, CA). A LKB 1282 Compugamma Universal Gamma Counter was used to count activities.

3.1.3 Methods

3.1.3.1 Human Serum Albumin Labeling with Iodine-125

The HSA iodination procedure was that provided by Pierce. One Iodobead with an oxidation capacity of 0.55 μ moles/bead was added to a vial containing 0.25 ml of 0.01 M PBS buffer, pH 7.2. Two microlitres of Na^{125}I (0.006 mg/ml) with a specific activity of 0.05 MBq/ μ g and 0.25 ml of HSA in PBS buffer (0.8 mg/ml) were added to the vial and the reaction was allowed to continue for 10 minutes at room temperature. To check the labeling efficiency of the iodination reaction, samples were taken from the reaction flask at regular intervals and added to tubes containing 1 ml rabbit albumin (2 mg/ml). One ml of trichloroacetic acid (TCA, 0.5M) was added to the tubes while mixing gently to allow aggregation and precipitation of the proteins. The tubes were centrifuged and 1 ml of supernatant was removed. The supernatant (S) and the protein pellets (P) were counted in a gamma counter. Efficiency of the reaction was calculated using the equation:

$$\text{Efficiency} = (\text{P-S})/(\text{P+S}) \times 100. \quad [3.1]$$

Once the efficiency of the reaction was more than 70%, the Iodobead was removed to stop the reaction. To remove unreacted Na¹²⁵I and to change the buffer from the reaction buffer (0.01 M PBS pH 7.2) to the buffer that was used for adsorption experiment (0.001 M PBS pH 7.2) the reaction mixture was loaded into the Sephadex size exclusion column. Fractions were collected and counted for maximum activity and those with albumin were pooled. The labeled albumin was stored in small quantities at -4° C.

3.1.3.2 Human Serum Albumin Stock Preparation

The HSA stock was prepared by diluting ¹²⁵I-HSA with unlabeled HSA. Three 1 µl aliquots of this HSA stock were counted in a gamma counter. Two 5 µl aliquot of the HSA stock were added to tubes containing 1 ml rabbit albumin (2 mg/ml), then 1 ml of TCA (0.5M) was added to each tube while mixing gently to allow aggregation and precipitation of the proteins. The tubes were centrifuged and 1 ml of supernatant was removed. The supernatant (S) and the protein pellets (P) were counted in the gamma counter. The fraction of protein bound counts for the HSA stock, F, was calculated using the equation: $F = (P-S)/(P+S) \times 100$. The protein concentration was calculated from the absorbance and the extinction coefficient of HSA at 278 nm (i.e., absorbance unit of 0.667 for BSA at 278nm = 1 mg/ml). Specific activity of the albumin stock was calculated using the formula:

$$SA = (P F \times 10^3) / C \quad [3.2]$$

SA= specific activity (DPM/mg)

P= protein stock count average (CPM /µl)

F= Fraction of counts bound in the HSA stock

C= γ -counter efficiency = 0.77

3.1.3.3 HSA Adsorption to the Latex Grafted with N, N-dimethacrylamide

Adsorption of HSA on the latex grafted with poly(N,N-dimethylacrylamide) was measured as follows:

A latex stock was prepared by addition of the grafted latex to 10 mM PBS, pH 7.2. The latex content of the latex stock was determined by freeze drying. Aliquots of 0.5 g of the latex from the latex stock were placed in micro centrifuge tubes. Different amounts of radioactive HSA (from HSA stock) were added to the tubes by volume and made up to 0.750 ml with PBS. The mixture was equilibrated for 30 minutes at room temperature while mixing on a rotating table. The mixture was centrifuged at 3000 x g for 2.5 minutes then the supernatant carefully removed without disturbing the pellet. Two 100 μ l aliquots of the supernatant were removed and counted to determine the equilibrium concentration. The pellet was washed by resuspending in 0.60 ml of PBS buffer (10 mM, pH 7.2). The suspension was placed on the rotating mixer for 10 minutes and centrifuged again at 3000 x g for 2.5 minutes. An aliquot of the supernatant was again counted to determine the amount of free HSA. The pellet was washed two more times with PBS, counting 100 μ l of the supernatant. Then the pellet and the pipette tip that was used for washing were counted. If the count in cpm from the last wash supernatant was much smaller than pellet plus pipette tip count (> 1000 times smaller), washing was not continued. Typically, three washes of the pellet removed virtually all of the free protein. The pellet was transferred to a new micro

centrifuge tube and the old micro centrifuge tube that was used for the protein adsorption experiment was counted to determine the amount of the protein adsorbed to the tube itself. Six microhematocit capillary tubes were filled with the washed latex from the adsorption experiment. The tubes were centrifuged at 13,000 x g for 10 minutes in a microhematocrit centrifuge (IEC, Needham Heights, MA). Pellet and supernatant heights in the capillary were accurately measured with a small scale ruler. The capillary tubes were cut with a diamond pen at the pellet-supernatant interface and each part counted in the gamma counter.

For each grafted latex, a calibration curve of latex volume fraction vs latex weight was produced (Figure A.2, Appendix). A series of latex suspensions was prepared by serial dilution of a latex stock. The weight % of the latex stock was determined by freeze drying. For each latex suspension, six microhematocrit tubes were filled and centrifuged. The volume fraction of each tube was measured by measuring the height of the pellet and supernatant. The average diameter of the tube was determined by weighing 10 capillary tubes filled with water. Using the capillary tubes weight, density of the water at 22° C and the height of water in cm, an average diameter of the capillary tube was calculated. The calculated diameter was in agreement with the manufacturer's specifications. The weight of the latex in the tube was calculated by multiplying the weight of the latex suspension in the tube by the latex weight %.

Using the calibration curve of latex volume fraction versus latex weight, the amount of the latex per gram for the six microhematocrit capillary tubes filled with the washed latex was determined. The amount of the adsorbed protein in mg/m² was

calculated from the pellet counts and the latex weight obtained from the calibration curve. The values for protein adsorption in the six capillary tubes were averaged and plotted against equilibrium concentration. For comparison, protein adsorption was also calculated directly from the pellet counts, assuming that latex was not lost during the washing process and plotted against equilibrium concentration (Figure A.3, Appendix).

The values of apparent dissociation constants K_d and adsorption maxima n were determined by non-linear curve fitting of the adsorption data to a hyperbolic curve ($y = nx / (k_d + x)$) using Origin 4.1 program (Microcal Software, Inc., Northampton, MA).

3.1.4 Results

HSA adsorption to polystyrene latex grafted with N,N-dimethylacrylamide calculated by the depletion and direct methods are shown in Figures 3.1 and 3.2 for four grafted and one non-grafted latex. The adsorption isotherm of HSA by the depletion method followed the same trend as the isotherm obtained by the direct method. The adsorption maximum values were slightly higher than those obtained by the direct method due to the loss of HSA that absorbed reversibly to the latex and was removed during washing. The maximum adsorption values and the apparent dissociation constant for each adsorption isotherm were measured by non-linear curve fit and presented in Table 3.1 for both methods.

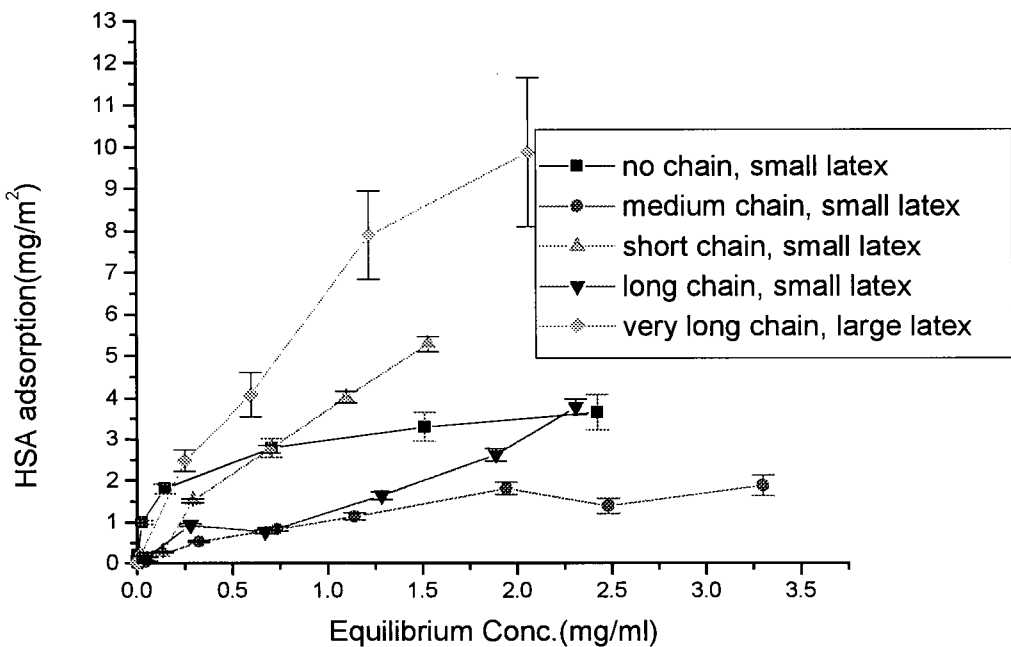


Figure 3.1 Human serum albumin adsorption to FS4 (■, no chain, small latex), FS3AG(●, medium chain, small latex), FS3AG2(▲, short chain, small latex), FS3AG3(▼, long chain, small latex) and FS4P2P'AG(◆, very long chain, large latex) by the depletion method. Errors were computed by propagation of estimated measurement errors of initial ($\pm 5\%$) and equilibrium concentrations ($N = 3$).

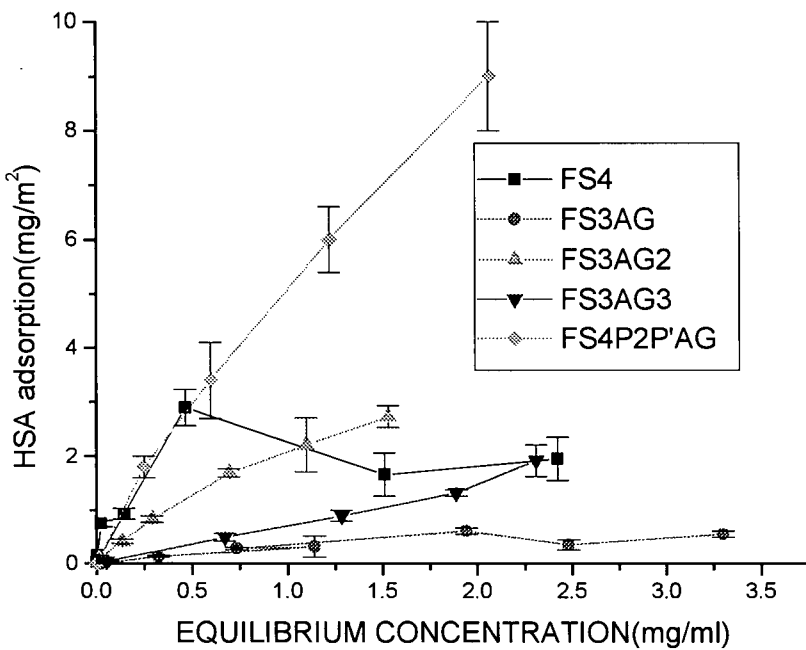


Figure 3.2 Human serum albumin adsorption to FS4 (■, no chain, small latex), FS3AG(●, medium chain, small latex), FS3AG2(▲, short chain, small latex), FS3AG3(▼, long chain, small latex) and FS4P2P'AG(◆, very long chain, large latex) by the direct method in microhematocrit capillary tubes. (N = 6, error bars are ± one standard deviation)

Latex	K_d (mg/ml)		n (mg/m ²)		Initial Slopes (ml/m ²)	
	Depletion	Direct	Depletion	Direct	Depletion	Direct
FS4 (8)*	0.13±.03	0.07 ± 0.03	3.6 ± 0.2	1.7 ± 0.1	29 ± 7	25 ± 10
FS3AG(12) *	1.4 ± 0.4	1.2 ± 0.7	2.6 ± 0.3	0.7 ± 0.22	1.9 ± 0.5	0.6 ± 0.4
FS3AG2 (7)*	-	1.7 ± 0.2	-	5.7 ± 0.3	3.5 ± 0.5	3.4 ± 0.4*
FS3AG3(7)*	-	-	-	-	1.6±0.3*	0.71±0.02*
FS4P2P'AG (5)*	1.9 ± 0.5	4.0 ± 0.8	19 ± 3	26 ± 4	10 ± 3	7 ± 2

* measured by linear fit

* (N) = number of data points

**Table 3.1- Dissociation constants K_d and absorption maxima n of latexes FS4
(no chain, small latex), FS3AG (medium chain, small latex), FS3AG2
(short chain, small latex), FS3AG3 (long chain, small latex),
FS4P2P'AG (very long chain, large latex) by direct and depletion
methods. A hyperbola curve was fitted on data set putting equal
weight on every data point. Errors are ± one standard deviation of the
mean.**

For the non-grafted latex FS4, the graph of HSA adsorption versus equilibrium concentration plateaued at very low equilibrium concentrations. The low value of the apparent dissociation constant K_d of this latex indicated that the HSA adsorption was very strong. The grafted latexes had higher K_d values than non-grafted latex indicating that the HSA had a lower apparent affinity for these latexes. FS3AG with medium

grafted chain length adsorbed the least HSA. FS3AG2 with a short grafted chain lengths had a larger adsorption maximum than the non-grafted latex. FS3AG3 with long grafted chain length had a lower adsorption maximum than the non-grafted latex but it had larger adsorption maximum than FS3AG with a medium grafted chain lengths. The maximum adsorption of HSA was to the largest latex, F4P2P'AG (3.5 microns in diameter compared to 0.79 micron for the other latex) with very long grafted chain lengths.

The direct method adsorption results in microhematocrit capillary tubes were compared with those determined directly with the counts from the pellet in the origin tube, assuming that latex was not lost during the washing process (Figure A.3, Appendix). The values obtained for adsorption by the direct method should be different than those obtained by counting the pellet if significant amount latex was lost during washing. The results of the two methods were in agreement within experimental error, indicating that the amount of the latex lost during the wash steps was not significant enough to change the adsorption isotherm.

3.1.5 Discussion

The results of the adsorption experiments can be explained if we consider the three major forces which are involved.

E= Entropic repulsion caused by the brush exclusion volume, probably independent of length for long chains; increases with surface density

G= Attractive forces between the HSA and N,N-dimethylacrylamide; increases with chain length and surface density

L= Attractive forces between the HSA and the latex

For the bare non-grafted latex, FS4, hydrophobic and electrostatic attractive forces between the latex and the protein are the likely causes of protein adsorption. However, for the grafted latexes, FS3AG, FS3AG3 and FS4P2P'AG, the magnitude of these forces likely becomes negligible due to the repulsive effect of the brush. Therefore, the driving force for adsorption of HSA onto these grafted latexes is the sum of the repulsive force of E and the attractive force of G . Both forces depend on the degree of penetration of the HSA into the grafted layer. If the repulsion is greater than attractive forces, HSA is excluded from the latex and if repulsion is less than attractive forces, HSA is adsorbed into the grafted polymer. It can be assumed that repulsion due to the grafted chains is approximately equal for these three grafted latexes because of their long brush and comparable chain separation. Consequently, the adsorption of HSA should increase with an increase in the brush length due to an increase in the attractive force G . FS3AG had a lower G due to the short brush length and a lower adsorption maximum (Table 3.1). FS4P2P'AG had a very large adsorption maximum due to the very long brush length. For FS3AG and FS3AG3, the effect of the repulsive force E was greater than the effect of the attractive force G , therefore the HSA was excluded and a lower adsorption maximum than the bare latex was observed; however, for FS4P2P'AG, the effect of attractive force G was bigger than repulsive force E , meaning more HSA was adsorbed by the grafted polymer than excluded and a higher adsorption maximum value than for the bare latex was observed.

For FS3AG2, the net force involved in the adsorption of HSA into the latex was the sum of the all three forces because of the short grafted brush. FS3AG2 had a lower K_d and larger adsorption maximum than non-grafted latex. At low equilibrium concentrations, HSA is adsorbed by the attractive forces of G and L and excluded by the repulsive force E due to the exclusion effect of the short brush. The grafted chains stretching into the solvent are the result of two opposing factors: the entropically unfavorable chain stretching due to the undesirable interaction of the polymer with the solvent and excluded volume interactions between polymer chains. The sum of these two factors determines the brush height at equilibrium. As the amount of free HSA in the bulk solution increases, the total free energy of the solvent in the bulk solution decreases, causing an osmotic pressure that removes the solvent trapped between the grafted polymer chains. Consequently, in the new equilibrium, the grafted polymer is compressed and the chain height is reduced. This could allow HSA to interact with the surface increasing adsorption. Therefore, for FS3AG2, at high concentration of HSA, the effect of attractive force L increases and the effect of repulsive force E decreases. Consequently, due to large attractive force (L and G) and low repulsive force (E), HSA adsorption to the FS3AG2 had a higher adsorption maximum than non-grafted latex.

Steels *et al.* (70) have investigated the interaction of chain polymers with a disk shaped solute using the numerical self consistent field theory for attractive chain-solute interaction ($\chi_{23}<0$). As the particles begin to move into the brush, favorable brush-particle contact energies dominate the interaction energy (Figure 1.2). The onset of the energetic repulsion does not occur until the disk penetrates inside the brush. The layer

position at which the onset of energetic repulsion exceeds that of favorable brush-particle attraction varies with the size of the disk, grafting density and the brush length. The layer position for the onset of repulsion varies approximately linearly with the brush Height, meaning longer chains repel the disk better. However because longer brush lengths have larger total favorable brush-particle interactions, it is suggested that very long flexible brushes may actually be less effective in reducing adsorption. This prediction agrees with the results obtained for the adsorption of the HSA to latex grafted with DMA. The adsorption of the HSA increased for the long chain of DMA.

3.2 The Nature of Adsorption of HSA to Poly(N,N-dimethylacrylamide)

To examine the nature of HSA adsorption to the grafted polymer, poly(N,N-dimethylacrylamide) is the result of hydrophobic interactions, the adsorbed HSA on latex FS4P2P'AG was washed with sodium dodecyl sulphate (SDS, 2.5%). After centrifugation, the pellet and supernatant were counted. The counts of supernatant and pellet in cpm/ml were plotted against the number of washes in Figure 3.4 and 3.5. Three washes of the pellet with PBS produced no significant change in the pellet and supernatant counts. When the pellet was washed with SDS (2.5%), the pellet counts decreased and the supernatant counts significantly increased indicating that HSA was removed from the latex surface. The second wash with SDS removed more HSA but less than the first wash. Hydrophobic interactions between the hydrophobic SDS and hydrophobic areas of HSA or between the SDS and the grafted polymer could be responsible for the removal of HSA during washing. Electrostatic interactions between the negatively charged SDS and the positively charged latex could also contribute to

the removal of HSA. SDS is highly denaturing to proteins and the denaturing could also contribute to the removal of HSA.

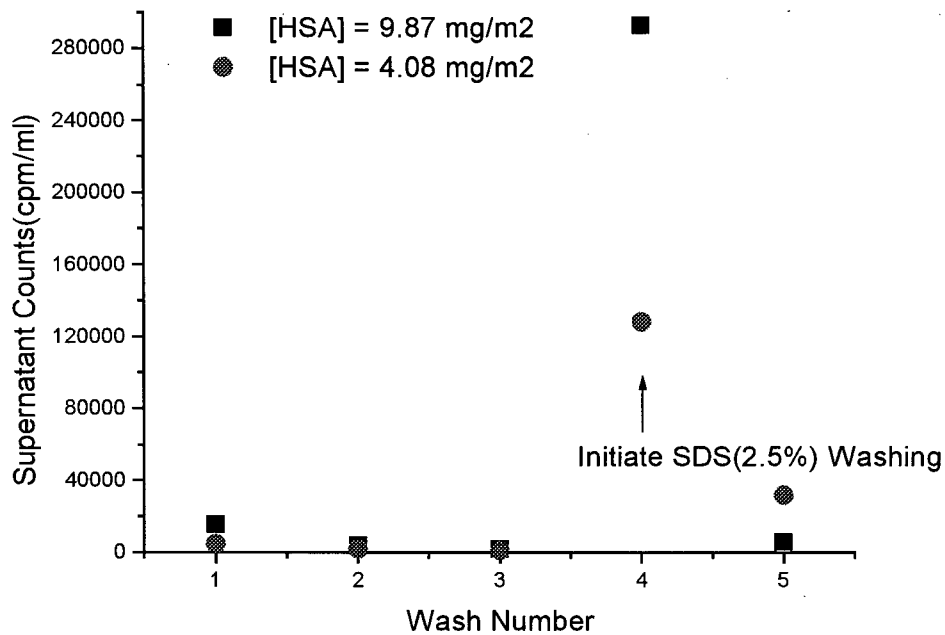


Figure 3.3- Plot of supernatant counts (cpm/ml) vs wash number.

HSA adsorbed to latex FS4P2P'AG at two different concentrations (measured by the depletion method) was washed three times with PBS, pH 7.2 and two times with SDS (2.5%) (N=1).

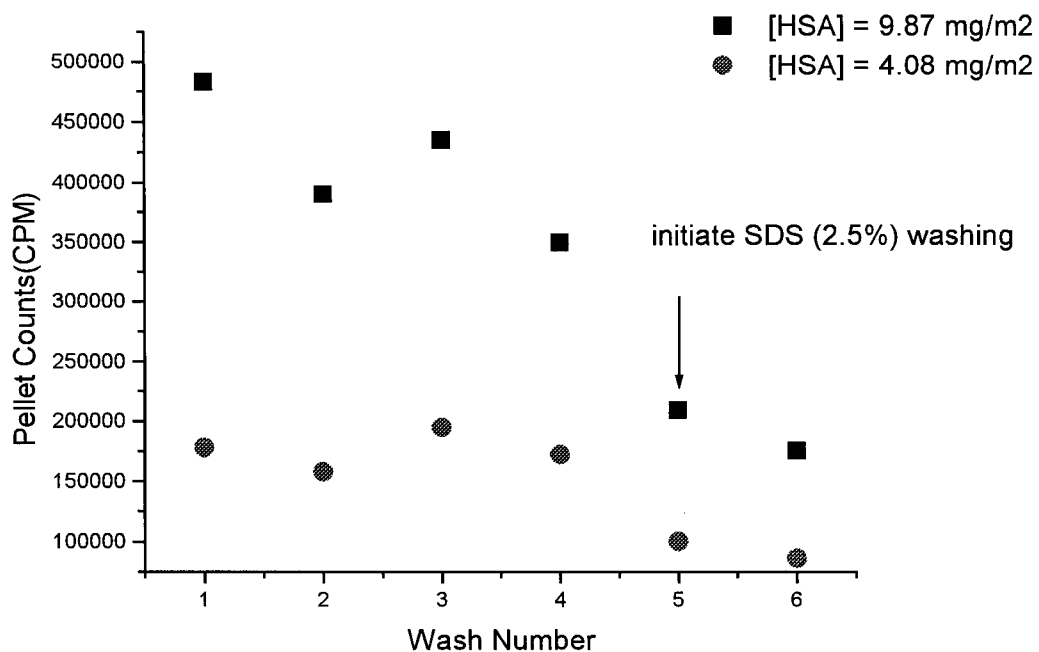


Figure 3.4- Plot of pellet counts (cpm/ml) vs wash number.

HSA adsorbed to latex FS4P2P'AG at two different concentrations (measured by the depletion method) was washed three times with PBS, pH 7.2 and two times with SDS (2.5%) (N=1).

3.3 Conclusion

The amount of human serum albumin (HSA) adsorbed to polystyrene latex grafted with different chain lengths of poly(N,N-dimethylacrylamide) was obtained by the direct and depletion methods. The results suggest that there was negative interaction energy between the poly(N,N-dimethylacrylamide) chains and HSA. It was also concluded that there is an optimal chain length where the repulsive force due to the excluded volume of the chain is greater than the attractive force. The longer brush lengths adsorbed more HSA due to the attraction forces between the chains and the HSA. The latex with shorter brush length adsorbed more HSA due to attraction forces between HSA and the latex.

Chapter 4: Entropic Interaction Chromatography with Poly(N,N-dimethylacrylamide) Grafted Latex

4.1 Introduction

Poly(N,N-dimethylacrylamide) brush grafted on polystyrene latex was used to examine the size exclusion property of the grafted polymer as predicted by Brooks and Müller(78).

4.2 Materials and Methods

The macromolecules used in this experiment were (MW, isoelectric point): human serum albumin (66000, 4.71), bovine insulin (6500, 5.3), myoglobin (16890, 6.99), fibrinogen (341000, 5.4), human IgG (156000, 7.3), keyhole limpet hemocyanin (KLH) (3×10^6). They were purchased from Sigma. Sodium nitrate (NaNO_3)(69) was purchased from Fisher. The polystyrene beads grafted with N,N-dimethylacrylamide were synthesized as described in chapter 3 (latex FS4P2P'AG). A stainless Steels HPLC column (Upchurch Scientific, Oak Harbor, WA) measuring 75 x 4.6 mm was packed with the grafted latex beads in distilled water under pressure and stored at 4°C. Prior to the experiment, water was displaced with the mobile phase, PBS pH 7.2. Protein solutions were prepared in PBS buffer pH 7.2 at a concentration of 1 mg/ml except myoglobin (0.5 mg/ml). Aliquots of 20 μl of each protein were loaded into the column at a flow rate of 0.5 ml/min and peaks were monitored by absorbance at 280 nm. The elution volumes of the KLH and sodium nitrate were considered as void volume (V_0) and total volume (V_t) of the column respectively.

4.3 Results

As discussed in chapter 3, human serum albumin binds to the grafted poly(N,N-dimethylacrylamide), therefore it was necessary to saturate the grafted latex beads with a protein prior to examining the size exclusion effect of the brushed polymer. The column was saturated by applying 20 μ l aliquots of the HSA solution (1 mg/ml) until the concentration of eluted HSA indicated by the area under HSA peak was constant (Figure 4.1). Increasing concentrations of HSA was also applied to the column and the concentration of eluted HSA indicated by the area under the HSA peak was measured (Figure A.4). The concentration of eluted HSA was linearly related to applied HSA concentration, indicating that the column was saturated.

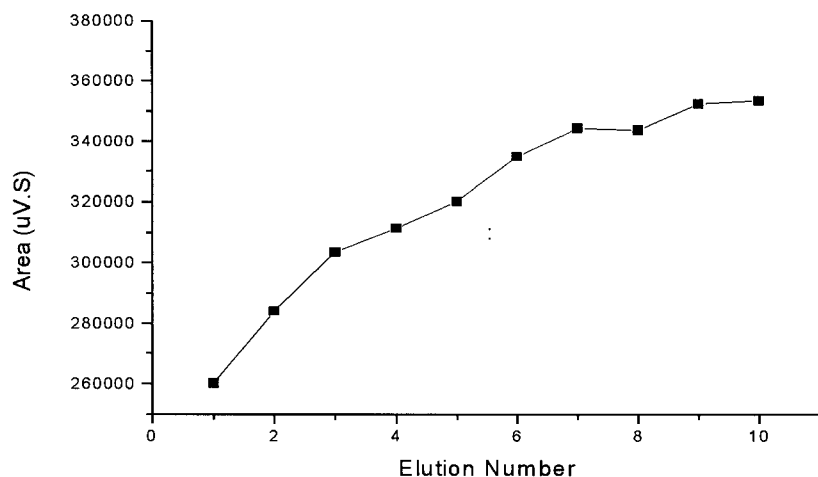


Figure 4.1- Saturation of the FS4P2P'AG with HSA (1 mg/ml) (N=1)

The size exclusion chromatography with the grafted latex FS4P2P'AG was carried out and results are shown in Figure 4.2.

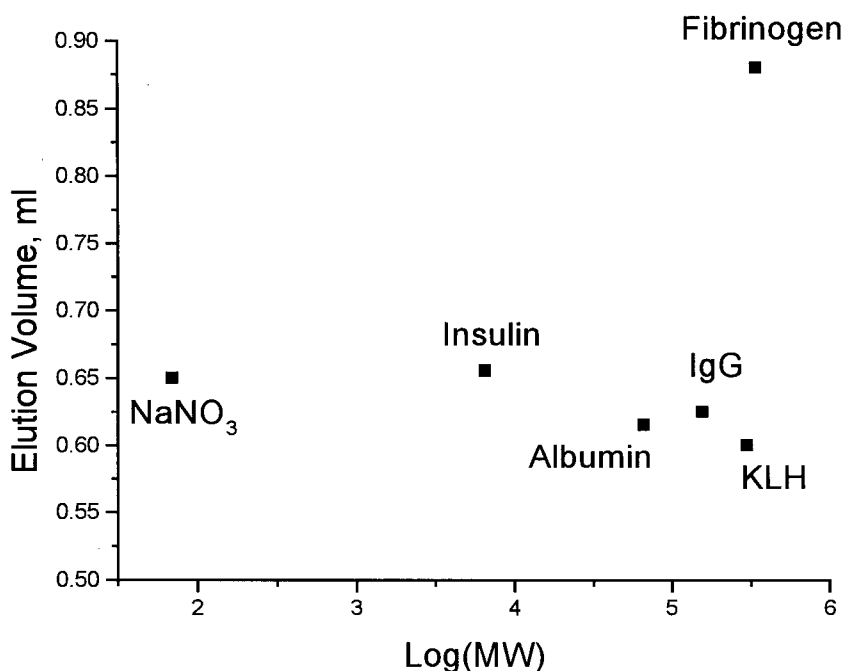


Figure 4.2- Entropic interaction chromatography with the polystyrene latex grafted with N,N-dimethylacrylamide (N = 5). Macromolecules (MW) were human serum albumin (66000), insulin (6500), human fibrinogen (341000), IgG(156000), keyhole limpet hemocyanin (3×10^6) and NaNO₃(69).

4.4 Discussion

Although a partial size-related separation was observed, the results are not conclusive enough to suggest that macromolecules can be separated by the entropic effect of the brush saturated with HSA. The data also suggest that fibrinogen has a specific affinity for the grafted beads.

4.4 Conclusion

Entropic interaction chromatography of polystyrene beads grafted with N,N-dimethylacrylamide was tested. The grafted polymer could not separate macromolecules according to their size as predicted because protein was adsorbed through hydrophobic interaction to the grafted poly(N,N-dimethylacrylamide) ($(\chi_{13}-\chi_{23}) \neq 0$).

Thesis Conclusion

Polystyrene latexes with an acrolein shell were synthesised for grafting of 2-methoxyethylacrylate and N,N-dimethylacrylamide by the cerium redox system. 2-methoxyethylacrylate could not be grafted by the cerium redox system due to high levels of solution polymerization. The monomer N,N-dimethylacrylamide was grafted to the latex with high efficiency. Human serum albumin adsorption to the latex grafted with poly(N,N-dimethylacrylamide) brush chains was examined. The result showed that HSA had affinity for grafted poly(N,N-dimethylacrylamide). When chains are long, HSA adsorption to the grafted chains dominates over chain exclusion, leading to a higher HSA binding than to bare latex. When the grafted chains are of medium length, the exclusion effect of the chain dominates over adsorption to the grafted polymer, leading to lower HSA binding than to bare latex. With short grafted chain, HSA adsorbs to both polystyrene latex and grafted polymer. The results were in general agreement with the numerical SCF theory.

References

- 1- Albanese A, R. Barbucci, J. Belleville, S. Bowry, R. Eloy, H.D. Lemke and L. Sabatini, *in vitro* Biocompatibility Evaluation of a Heparin Table Material (PUPA), Based on Polyurethane and Poly(amido-amine) Components, *Biomaterials*, 15, 2, 129-136 (1994)
- 2- Park K.D., T. Okano, C. Nojiri, and S. Wan Kim, Heparin Immobilization onto Segmented Polyurethane Surfaces—Effect of Hydrophilic Spacers. *Journal of Biomedical Materials Research*, 22, 977-992 (1988)
- 3- Ofosu F.A., M. A. Blajchman, G.J. Modi, L.M. Smith, M.R. Buchanan and J. Hirch. The Importance of Thrombin Inhibition for the Expression of the Anticoagulant Activities of Heparin, Dermatan Sulfate, Low Molecular Weight Heparin and Pentosan Polysulphate. *British Journal of Haematology* 60, 695 (1985)
- 4- Gin H, B. Dupuy, D. Bonnemaison-Bourignon, L. Bordenave, R. Bareille, M.J. Latapie, C.H. Baquey, J. H. Bezian, D. Ducassou. Biocompatibility of Polyacrylamide Microcapsules Implanted in Peritoneal Cavity or Spleen of the Rat Effect on Various Inflammatory Reaction *in vitro*. *Biomat. Art. Cells, Art. Org.*, 18(1), 25-42 (1990)
- 5- Fujimoto, K., H. Tadokoro, Y. Ueda and Y. Ikada, Polyurethane Surface Modification by Graft Polymerization of Acrylamide for Reduced Protein Absorption and Platelet Activation. *Biomaterials*, 14, 6, 442-447, (1993)
- 6- Merill E.W and E.W. Salzman, Polyethylene Oxide as a Biomaterial. *J. Am. Soc. Artif. Intern. Organs*, 6, 60 (1983)
- 7- Okano T, K Suzuki, N Yui, Y Sakuri and S Nakahama, Prevention of Changes in Platelet Cytoplasmic Free Calcium Levels by Interaction with 2-Hydroxyethylmethacrylate/Styren Block Copolymers Surfaces. *J. Biomed. Mater. Res.*, 27, 1519-1525 (1993)
- 8- Brauker J.H., V.E. Carr-Brendel, L.A. Martinson, J Crudele, W.D. Johnson, R.C. Johnson, Neovascularization of Synthetic Membranes Directed by Membrane Microarchitecture, *J. Biomed. Mater. Res.*, 29, 1517-1524 (1995)
- 9- Singhui R, A Kumar, G. Lopez, O. Stephan, G. Poulosz, D.C. Wang, G.M. Whitesides, D. Ingber, Engineering Cell Shape and Function, *Science*, 264, 696-698 (1994)
- 10- Ferguson G.S., M.K. Chaudhury, H. Biebuyck, G.M. Whitesides, Monolayers on Disordered Substrates: Self-Assembly of Alkyltrichlorosilanes on Surface-Modified Polyethylene and Poly(dimethyl Siloxane). *Macromolecules* 26, 5870-5875 (1993)

- 11- Jozefonuicz J, M. Jozefowicz: Review: Interactions of Biospecific Functional Polymers with Blood Proteins and Cells. *Journal of Biomedical Science Polymer Edition*, 1(3), 147-165 (1990)
- 12- Uyama Y, H. Tadakoro and Y. Ikada, Low-Frictional Catheter Materials by Photo-Induced Graft Polymerization. *Biomaterials*, 12, p71-73 (1991)
- 13- Desai N.P. and J.A. Hubbel, Biological Responses to Polyethylene Oxide Modified Polyethylene Terephthalate Surfaces, *J. Biomedical Materials Research*, 25, 829-843 (1991)
- 14- Haycox C.L. and B.D. Ratner, *In Vitro* Platelet Interactions in Whole Human Blood Exposed to Biomaterial Surfaces: Insights on Blood Compatibility, *J. Biomed. Mater. Res.* 27: 1181 (1993)
- 15- Eberhart, R.C. In: *Proteins at Interface: Physiochemical and biochemical studies*, J.L. Brash and T.A.Horbett, (1987)
- 16- Kang I, B.K. Kwon, J.H. Lee and H.B. Lee, Immobilization of Proteins on Poly(methylmethacrylate) Films, *Biomaterials*, 14(10), 787-92 (1993)
- 17- Golander C. And E. Kiss, Protein Adsorption on Functionalized and ESCA-Characterized Polymer Films Studied by Ellipsometry, *J. Coll. Interface Sci.* 121: 240 (1987)
- 18- Ertel, S.I., B.D. Ratner, T.A. Horbet, Radio Frequency Plasma Deposition of Oxygen-Containing Films on Polystyrene and Poly(ethylene terephthalate) Substrates Improves Endothelial Cell Growth. *J. Biomed. Mater. Res.*, 24(12) 1637-1659 (1990)
- 19- Kauzmann W. Some Factors in the Interpretation of Protein Denaturation, *Adv. Protein Chem* 14:1 (1959)
- 20- Bing D. H., The Chemistry and Physiology of The human Plasma Proteins Albumin: Sequence Evolution and Structural Models In: *The Chemistry and Physiology of the Human Plasma Proteins* Edited by Pergamon Press, NY, 1978, 23-41
- 21- Brown, J.R., Serum Albumin: Amino Acid Sequence In: *Albumin Structure, Function and Uses* Eds. Rosenoer, V.M., Oratz, M., and Rotchhschild, M.A. Pergamon Press (1997)
- 22- Brown, J.R., Structure of Bovine Serum Albumin. *Fed. Proc. (Fed. Am. Soc. Exp. Bio.)*, 34, 391 (1975)

- 23- Carter, D.C, S.H. Xiao-Min Munson, D.G. Twigg, K.M. Gernett, M.B. Broom and T.Y. Miller, Three Dimensional Structure of Human Serum Albumin. *Science* 224, 1195-1198 (1989)
- 24- Aoki, K. and J.F. Foster, Electrophoretic Behavior of Bovine Plasma Albumin at Low pH. *J. Am. Chem. Soc.*, 79, 3386-3396 (1963)
- 25- Sogami, M. and J.F. Foster, Microheterogeneity as the Explanation for Resolution of N and F Forms of Plasma Albumin in Electrophoresis and Other Experiments. *J. Biol. Chem.* 238, pc2245-pc2247 (1963)
- 25(b)- Foster, J.F. (1990). *Plasma Albumin in the Plasma Proteins*. Putman F.W. E.D; Academic Press N.Y. (1960)
- 26- Sogami, M. and J.F. Foster, Isomerization Reaction of Charcoal- Defatted Bovine Albumin. The N-F Transition and Acid Expansion. *Biochem*, 7, 2172-2182 (1968)
- 27- Walleuk, K., Reversible denaturation of human Serum Albumin by pH, Temperature and Guanidine hydrochloride Followed by Optical Rotation. *J. Biol. Chem.*, 248, 2650-2655 (1973)
- 28- Yutani K., K Ogasahara, K Sugino and A Matsusshiro, Effect of a Single Amino Acid substitution on Stability of Conformation of a Protein. *Nature (Lond.)*, 267, 274-275 (1977)
- 29- Hartley R.W.Jr., E.A. Peterson and H.A. Sober, The Relation of Free Sulphydryl Groups to Chromatographic Heterogeneity and Polymerization of Bovine Serum Albumin, *Biochemistry*, 1, 60-68 (1962)
- 30- Andersson L.O., The Heterogeneity of Bovine Serum Albumin. *Biochim. biophys. Acta*, 117, 115-133 (1966)
- 31- Everett D.H., Why are Colloidal Dispersions Stable? I Basic Principles In: *Basic Principles of Colloid Science*, Edited by the Royal Society of Chemistry, London, 16-28 (1988)
- 32- Israel achvilli J.N. and B.W. Ninham, Intermolecular Forces. The Long and Short of It. *J. Colloid Interface Sci.*, 58, 14 (1977)
- 33- Napper, D.H., Colloid Stability, *Ind. Eng. Chem. Prod. Develop.*, 9(4), 467 (1970)
- 34- Ottewill, R.H. The Stability and Instability of Polymer Latices In: *Emulsion polymerization*, Edited by Piirma, I. New York: Academic Press, 1987

- 35- Buscall, R and Ottewill, R.H. The Stability of Polymer Latices In: *Polymer Colloids* Edited by Buscall, R., Corner,T. and Stageman,J.F. London: Elsevier Applied Sciences, p141-218, 1974
- 36- Napper, D.H., *Polymeric Stabilization of Colloidal Dispersions*, Academic Press: New York (1983)
- 37- Kang, E.T, K.G. Neoh, K.L. Tan, Y. Uyama, N. Morikawa and Y. Ikada, Surface Modification of Polyaniline Films by Graft Copolymerization. *Macromol.* 25: 1959-1965 (1992)
- 38- Colloid-Polymer Interactions. Particulate, Amphiphilic, and Biological Surfaces, Washington, DC: American chemical society, PP.423 (1993)
- 39- Vincent, B., The Stability of Solid/ Liquid Dispersions in Presence of Polymers, In: *Solid /Liquid Dispersions*, Chap.7. Ed. Tadros Th. F. (Academic Press. London) (1987)
- 40- Russel W.B., D.A. Saville and W.R. Schowalter, Electrostatic stabilization In: *Colloidal Dispersions*, edited by Cambridge University Press, Cambridge, 88-126 (1989)
- 41- Salzman, E.W and E.W. Merill, Interaction of Blood with Artificial Surfaces In: *Homeostasis and Thrombosis, Basic Principles and Clinical Practice*, (2nd ed.) Colman, R.W., Hirsh, J Marder, V, V and Salzman, E.E (Eds). J.B Lipincott Company, Philadelphia, 1335-47 (1987)
- 42- Horbett T.A. and J.L. Brash, Proteins at Interfaces: Current Issues and Future Prospects In: *Proteins at Interfaces: Physiochemical and Biomedical Studies*, Brash, J. L. and Horbett, T.A.(Eds). American Chemical Society, Washington D.C., 1-33 (1987)
- 43- Packham M.A, G. Evans, M.F. Glynn and J.F. Mustard. The Effect of Plasma Proteins on Interaction of Platelets with Glass Surface. *J. Lab and Clin. Med.* 73(4), 686-697 (1969)
- 43(b)- Mulvihill, J.N., A. Faradji, F. Oberling and J.P. Cazenave, Surface Passivation by Human Albumin of Plasmapheresis Circuits Reduces Platelet Accumulation and Thrombus Formation. Experimental and Clinical Studies, *J. Biomed. Mater. Res.*, 24, 155-63 (1990)
- 44- Zucker, M.B. and L. Vroman, Platelet Adhesion Induced by Fibrinogen Adsorbed onto Glass. *Proc. Soc. Exp. Bio. Med.* 131 318-320 (1969)

- 45- Lambrecht, L.K., B.R. Young, R.E Stafford, K Park, R.M. Albrecht, D.F Mosher and S.L. Cooper, The Influence of PreadSORBED Canine von Willebrand Factor, Fibronectin and Fibrinogen on *ex vivo* Artificial Surface Induced Thrombosis, *Thromb. Res.*, 41, 99-117 (1986)
- 46- Kaplan, A.P. and M. Silverberg, The Coagulation-Kinin Pathway of human Plasma, *Blood*, 70, 1-15 (1987)
- 47- Guyton, A.C., Immunity and Allergy In: *Textbook of Medical Physiology*, edited by W.B. Saunders Company, Philadelphia, 60-70 (1986)
- 48-Lyman D.J., L.C. Metcalf, D. Albo Jr., K.F. Richards, and J. Lamb, The Effect of Chemical Structure and Surface Properties of Synthetic Polymers on the Coagulation of Blood. III. *in vitro* Absorption of Proteins on Polymer Surfaces, *Trans. Amer. Soc. Artif. Int. Organs*, 20, 474-478 (1974)
- 49- Mulzer, S. R. and J.L. Brash, Identification of Plasma Proteins Adsorbed to Hemodialysis During Clinical use. *J. Biomed. Mater. Res.*, 23, 1483, (1989)
- 49(b)- Damme H.S.V and J.Feijen, Protein Adsorption Polymer- Liquid Interfaces Using Series of Polymers with Varying Hydrophilicity, Charge and Chain Mobility In: *Modern Aspect of Protein Adsorption on Biomaterials*, Edited by Kluwer Academic Publishers, 55-63 (1991)
- 50- Vroman, L. Summation: Protein at the Interface. *Federation Proceedings*, 30(5): 1703-4 (1971)
- 51-Vroman L., A.L. Adams, M. Klings, Interaction Among Human Blood Proteins at Interfaces, *Federation Proceedings*, 30 (5), 1494-1502 (1971)
- 52- Haynes C.A. and W.Norde, Globular Proteins at Solid/Liquid Interfaces Colloids and Surfaces B: *Biointerfaces*. 2: 517-566 (1994)
- 53- Nemethy G. and H.A. Scheraga, Structure of Water and Hydrophobic Bonding in Proteins, II Model for the Thermodynamic Properties of Aqueous Solution of Hydrocarbons, *J. Chem. Phys.* 36: 3401 (1962)
- 54- Norde, W. and J.Lyklema, Thermodynamic of Protein Adsorption, *J. Colloid Interface Sci.* 71: 350 (1979)
- 55- Schoroën, C.G.P.H., M.A. Cohen Stuart, K. van der Voort Maarschalk, A. van der Padt and K. van't Reit, Influence of PreadSORBED Block Copolymers on Protein Adsorption: Surface Properties, Layer Thickness and Surface Coverage, *Langmuir*, 11, 3068-3074 (1995)

- 56- Golander, C.G., J.N. Herron, K. Lim, P.Claesson, P. Stenius and J.D. Andrade, Properties of Immobilized PEG Films and The Interaction with Proteins: Experiments and Modeling, *Poly(Ethylene Glycol) Chemistry: Biotechnical and Biomedical Applications* (J.M. Harris, ed.) Plenum Press: New York, 221-245 (1992)
- 57- Andrade, J.D. and V. Hlady, Protein Adsorption and Materials Biocompatibility: A Tutorial Review and Suggested Hypotheses, *Advances in Polymer Science* (K. Dušek, ed.) Springer-Verlag: Berlin, 1-63 (1986)
- 58- de Gennes, P.-G., Scaling Theory of Polymer Adsorption, *J. Phys. (Paris)*, 37, 1443-1452 (1996)
- 59- Janzen J., X. Song and D.E. Brooks, Interfacial Thickness of Liposomes Containing Poly(ethylene glycol)- Cholesterol From Electrophoresis, *Biophysical Journal*, 70 313-320 (1996)
- 60- Ikada Y. and E. Kulik, *In Vitro* Platelet Adhesion to Nonionic and Ionic Hydrogels with Different Water Contents, *Journal of Biomedical Materials Research*, 30, 295-304 (1996)
- 61- Kuhn. über Die Gestalt Fadenförmiger Moleküle in Lösungen. W. *Kolloid Z.* 68:2, (1934)
- 62- Flory, P., *J. Principles of Polymer Chemistry*. Ithaca, NY: Cornell University Press (1953)
- 63- de Gennes, P.-G. *Scaling Concepts in Polymer Physics*. Ithaca. NY. Cornell University Press. (1979)
- 64- Fleer, G.J., M.A.Cohen-Stuart, J.M.H.M. Scheutjens, T. Cosgrove, B Vincent *Polymers at Interfaces*, Chapman and Hall: London (1993)
- 65- de Gennes, P.-G., Scaling Theory of Polymer Adsorption *J. Phys (Paris)* 37, 1443-1452, (1976)
- 66- Alexander, S., Adsorption of Chain Molecules with a Polar Head: A Scaling Description, *J. Phys. (Paris)*, 38, 977-982, (1977)
- 67- Jeon S.I., J.H.Lee, J.D.Andrade and P.-G. de Gennes, Protein-Surface Interactions in The Presence of Polyethylene Oxide I. Simplified Theory. *J. Colloid Interface Sci.* 142(1), 149-158, (1991a)
- 68- Subramanian, G., D.R.M Williams and P.A. Pincus, Escape Transitions and Force Laws For Compressed Polymer Mushrooms. *Europhysics Letters*, 29(4), 285-290 (1995)

- 69- Szleifer I., Protein Adsorption on Surfaces with Grafted Polymers: A Theoretical Approach, *Biophysical Journal*, 72, 595-612 (1995)
- 70- Steels, B.M., Analysis of Interaction Between Finite-Sized Particles and Terminally Attached Polymer Using Numerical Self- Consistent-Field Theory, *Masters Thesis*, University of British Columbia (1997)
- 71- Scheutjens, J.M.H.M and G.J. Fleer, Statistical Theory of the Adsorption of Interacting Chain Molecules. 2. Train, Loop and Trail Size Distribution, *J. Phys. Chem.*, 84, 178-190 (1980)
- 72- Scheutjens, J.M.H.M and G.J. Fleer, Statistical Theory of the Adsorption of Interacting Chain Molecules. 1. Partition Functions, Segment Density Distribution and Adsorption Isotherms, *J. Phys.Chem.* 83, 1619-1635 (1979)
- 73- Flory, P., Thermodynamics of High Polymer Solutions, *J. Chem. Phys.*, 10, 51-61 (1942)
- 74- Flory, P. *Principles of Polymer Chemistry*. Cornell University Press: Ithaca, NY (1953)
- 75- Huggins, M.L., Some Properties of Solutions of Long Chain Compounds. *J. Phys. Chem.*, 46, 151-158 (1942)
- 76- Cosgrove, T., T.Heath, B.VanLent, F.Leemakers and J.Scheutjens. Configuration of Terminally attached Chains at the Soild/Solvent Interface: Self-Consistent Field Theory and a Monte Carl Model, *Macromolecules*, 20, 1692-1696 (1987a)
- 77- Leermakers, F.A.M. and J.M.H.M. Scheutjens, Statistical Thermodynamics of Association Colloids. I . Lipid Bilayer Membranes, *J. Chem. Phys.*, 89(5), 3264-3274 (1988)
- 78- Brooks D.E. and W. Müller. Size-Exclusion Phases and Repulsive Protein Polymer Interaction/Recognition. *Journal of Molecular Recognition*. 9, 697-700 (1996)
- 79- Porath J and P. Flodin, Gel Filteraction: A Method for Desalting and Group Seperation, *Nature* 183, 1657-1659 (1959)
- 80- Porath J., Some Recently Developed Fractionation Procedure and Their Application to Peptide and Protein Hormones. *Pure. Appl. Chem.* 6, 233-244 (1963)
- 81- Hritcu, D. Synthesis and Characterization of Cationic Latex Bearing Grafted Chains, *Ph.D Thesis*, University of British Columbia, (1998)

- 82- Goodwin, J.W., R.H. Ottewill and R.Pelton, Studies on The Preparation and Characterization of Monodisperse Polystyrene Latices, III Preparation Without Added Surfactant. *Colloid & Polymer Sci.* 252, 463-471 (1974)
- 83- Blaakmeer, J. and G.J.Fleer. Synthesis of Polystyrene Latex with a Positive, pH Independents, Surface Charge, *Colloids Surf.* 36: 439-447 (1989)
- 84- Yan, C. X. Zhang, Z.Sun, H. Kitano, N. Ise, Poly(styrene-co-acrolein) Latex Particles: Copolymerization and Characteristics. *J. Appl. Polym Sci.*, 40: 89-98 (1990)
- 85- Seaman, G.V.F., Electrokinetic Behavior of Red Cells. In: *Blood Cell*, Edited by D.M. Surgenor. New York: Academic Press, 1135-1229 (1975)
- 86- Bergström K and K. Holmberg. Reduction of Fibrinogen Absorption on PEG-Coated Polystyrene Surfaces. *Journal of Biomedical Materials Research*, 26, 779-790 (1992)
- 87- Nojiri C., T. Okano, H. A. Jacobs, K. D. Park, S. F. Mohammad, D. B. Olsen, and S. W. Kim, Blood Compatibility of PEG Grafted Polyurethane and HEMA/Styrene Block Copolymer Surfaces. *Journal of Biomedical Materials Research*, 24, 1151-1171 (1990)
- 88- Chung-Li Y, J.W. Goodwin and R.H. Ottewill. Studies on the Preparation and Characterization of Monodisperse Polystyrene Latices. *Progr. Colloid and Polymer Sci.* 60, 163-175 (1976)
- 89- Hritcu D, W. Müller and D.E. Brooks, Poly(styrene) Latex Carrying Cerium(IV)-Initiated Terminally Attached Cleavable Chains: Analysis of Grafted Chains and Model of the Surface Layer, *Macromolecules*, 32, 565-573 (1999)
- 90- Müller, W., U.S. Pat. 5453186, (1995)
- 91- Mino, G., S.Kaizerman, E. Rasmussen, A New Method For Preparation of Grafted Copolymers. Polymerization Initiated by Ceric Ion Redox Systems. *J. Polym. Sci: Polym. chem. Ed.*, 38, 393-404 (1959)
- 92- Panda, A. and B.C. Singh, Graft Copolymerization of Acrylic Acid onto Biomedical Polyvinyl Alcohol Initiated by Ce(IV)- Glucose Redox System: Part 2, *Poly.- Plast. Technol. Eng.*, 35(3), 487-496 (1996)
- 93- Wallace, L.A. and D.G. Young. Graft Polymerization of Kinetics of Ceric Nitrate-Dextran Redox Systems. *J. Poly. Sci.: Poly. Chem. Ed.* 4: 1179-1190, 1966

- 94- Athawale, V. D. and S. C. Rathi, Effect of Chain Length of The Alkyl Methacrylates on Graft Polymerization onto Starch Using Ceric Ammonium Nitrate as Initiator. *Eur. Polym. J.*, 33: 1067-1071 (1997)
- 95- Vroman, L., The Importance of Surfaces in Contact Phase Reactions. *Seminars Thromb. Haemostas.* 13, 79 (1987)
- 96- Privalov, P.L, Stability of Proteins: Small Globular Proteins, *Adv. Prot. Chem.* 33, 167 (1979)
- 97- Bull, H.B., Adsorption of Bovine Serum Albumin on Glass. *Biochem. Biophys. Acta* 19 464-471 (1956)

Appendix

Section 1:
Sample Calculation for Chain Separation, Degree of Polymerization, Radius of Gyration and Brush Height:

Chain separation, degree of polymerization, radius of gyration and brush height of the grafted latexes (table 2.4) were calculated with the following formulas:

For latex FS3AG

Aldehyde concentration (mole/g) in copolymer shell was determined by conductometric titration:

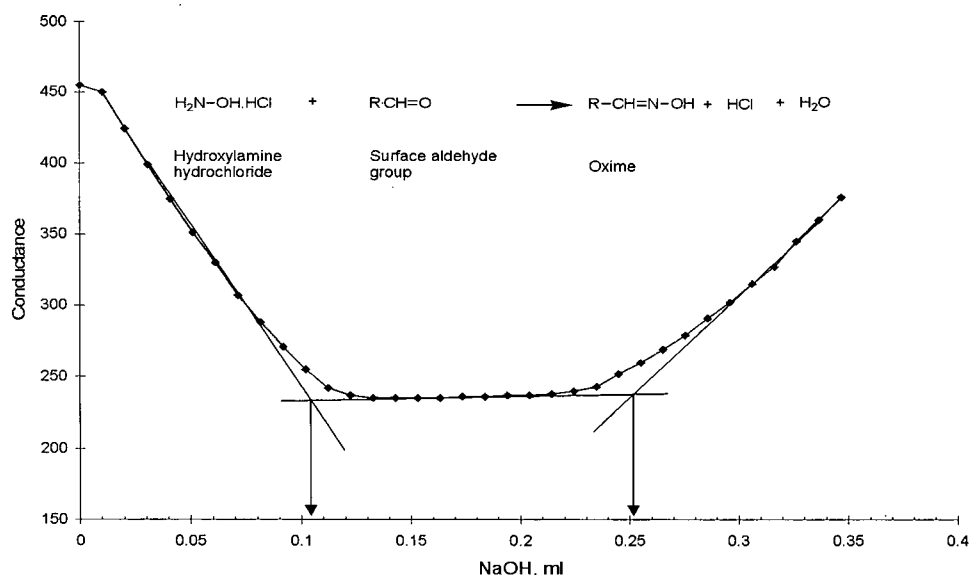


Figure A.1- Coductometric titration of latex FS3A to determine the amount of aldehyde groups on the surface. Latex FS3A covered with aldehyde functional groups was reacted with hydroxylamine hydrochloride. The HCl produced was titrated with NaOH (0.1 M).

Chain separation was calculated with the formula:

$$D = A^{1/2}, \text{ Å}$$

where D= chain separation on the surface of the beads, Å

A= area per aldehyde groups, Å^2 determined from titration graph

For FS3A:

$$A = 49 \text{ \AA}^2, D = 7 \text{ \AA}$$

Average degree of polymerization of the grafted chain (DP) was calculated with the formula:

$$DP = T / [-\text{CH=O}]$$

where T = polymerized N,N-dimethylacrylamide determined by HPLC or N_2 analysis (mole/g)

$[-\text{CH=O}]$ = aldehyde concentration determined from conductometric titration graph, mole/g

For FS3AG:

$$T (\text{HPLC}) = 0.0051, T (N_2) = 0.0038, [-\text{CH=O}] = 2.47 \times 10^{-5}$$

Radius of gyration(R_g) was estimated from(64):

$$R_g = a M_n^{1/2}$$

where M_n = Average molecular weight of the chains, g/mol ($M_n = 99.13 \text{ DP}$)
 $a = 261 \times 10^{-3}, \text{ \AA}$ (for poly(methylmethacrylate))

For FS3AG:

$$M_n (\text{HPLC}) = 2.05 \times 10^4 \quad M_n (N_2) = 1.52 \times 10^4$$

Brush height was calculated from(64):

$$h = (DP-1)(\sigma l^2)^{1/3}, \text{ \AA}$$

where σ = density of the grafted chains, \AA^{-2}

$l = 1.4$ = length of repeating unit in the polymer chain, \AA .

For FS3AG:

$$\sigma = A^{-1} = 0.02 \text{ aldehyde}/\text{\AA}^2$$

$$DP (\text{HPLC}) = 207, DP (N_2) = 154$$

Section 2:

Nitrogen Analysis of Latex Grafted with N,N-dimethylacrylamide

Nitrogen analysis of the grafted latexes FS3AG, FS3AG2 and FS3AG3 and non-grafted latex FS3A was carried out by SGS Canada Inc., Vancouver, BC. The difference between nitrogen content of the non-grafted and the grafted latex was used to calculate the degree of polymerization, the radius of gyration and the brush height (Table 2.4)

Latex	Non-grafted Latex (FS3A) Nitrogen (N) Content (%)	Grafted Latex Nitrogen (N) Content (%)
FS3AG	0.88	1.41
FS3AG2	0.068	0.13
FS3AG3	0.2	0.96

**Table A.1- Nitrogen analysis of non-grafted latex (blank) and grafted latex
(method AOAC 990.03).**

Section 3:

A calibration curve was used to measure the amount of the latex in the microhematocrit capillary tube as explained in section 3.1.3.3. A calibration curve was produced for each latex used in an albumin adsorption experiment (Table 3.1).

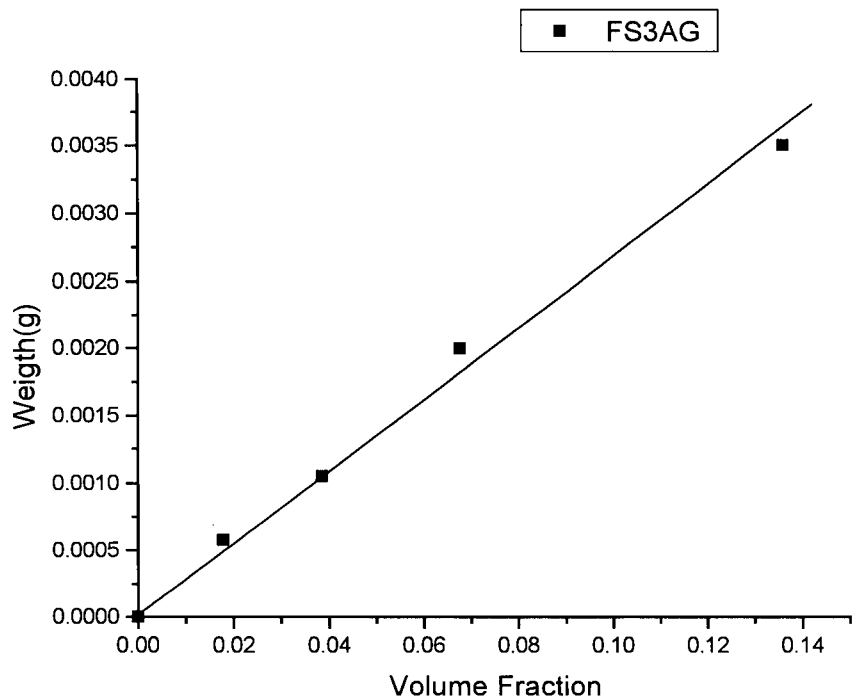


Figure A.2- Calibration curve of the grafted latex in the microhematocrit capillary tube ; weight of latex (FS3AG) vs volume fraction.

Section 4:

The amount of albumin adsorbed to the latex is calculated directly from the pellet counts and plotted against equilibrium concentrations (section 3.1.3)

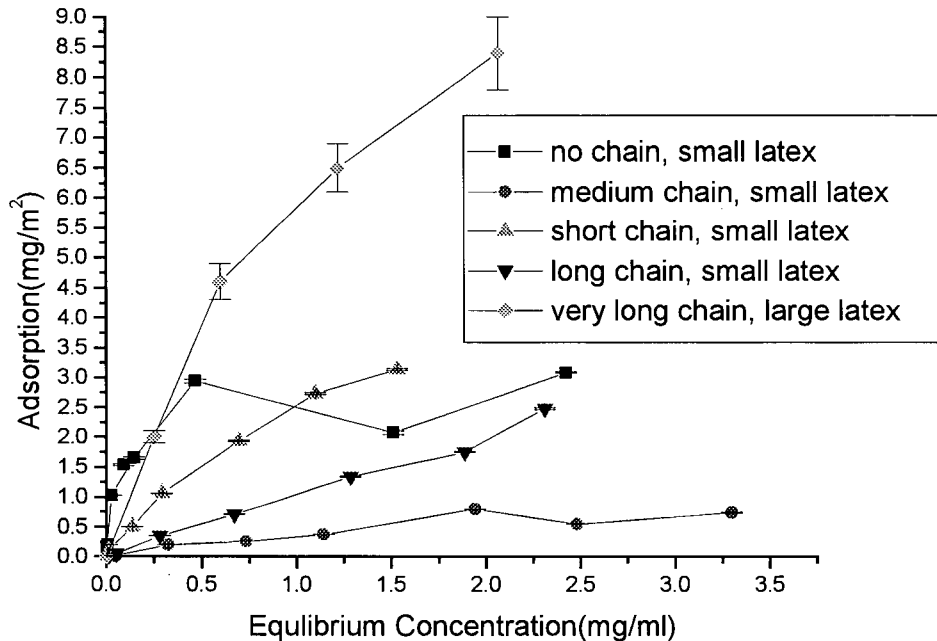


Figure A.3 - Human serum albumin adsorption to FS4 (■, no chain), FS3AG (●, medium chain, small latex), FS3AG2(▲, short chain, small latex), FS3AG3(▼, long chain, small latex) and FS4P2P'AG(◆, very long chain, large latex) by direct method (pellet counts). Errors were computed by propagation of estimated measurement error of the specific activity of the stock protein.

Section 5:

Albumin binds to the poly(N,N-dimethylacrylamide). Therefore the column filled with the latex grafted with poly(N,N-dimethylacrylamide) (FS4P2P'AG) was first saturated with HSA before size exclusion chromatography experiment (Chapter 4)

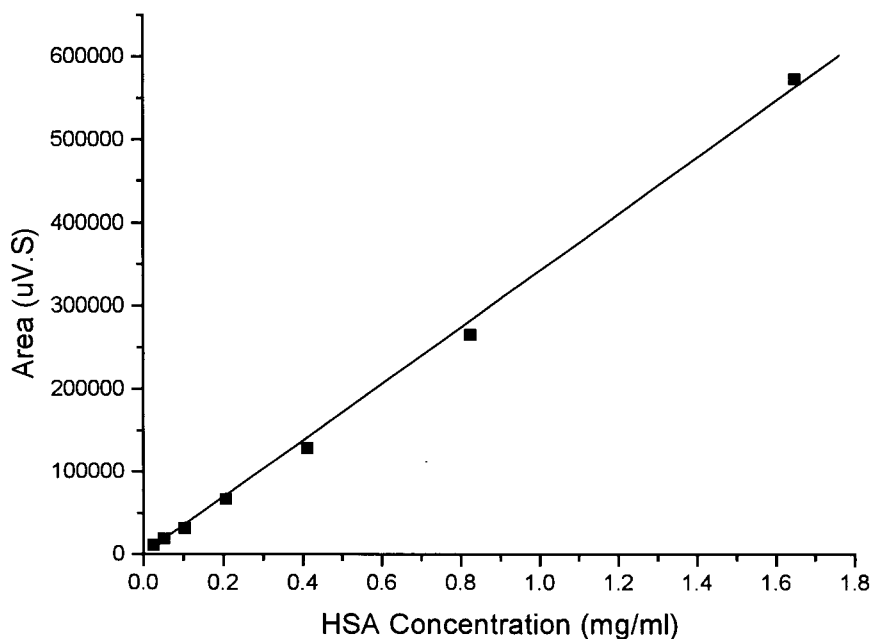


Figure A.4- Plot of HSA eluted from the column (area) vs HSA applied to the column. Chromatography column filled with the latex FS4P2P'AG was saturated by applying increasing concentrations of the HSA. (N = 1)